(CEUS) with Sonazoid can be expected to be useful also in ultrasound-guided percutaneous ablation, including RFA, because Kupffer imaging lasts usually for more than 60 min. However, there are few reports about the utility of Sonazoid as a contrast agent during RFA of HCC.[14,15]

The aim of the present study was to evaluate the utility of the contrast agent Sonazoid in ultrasound-guided percutaneous RFA of HCC in terms of HCC nodule detection. Overall facilitation of the ablation procedure was also evaluated by comparing the numbers of RFA sessions per treatment between RFA using CEUS with Sonazoid and matched historical controls that had used conventional US.

Methods

Patients

We analyzed a total of 716 HCC nodules in 316 consecutive patients who were admitted for RFA between July 2007 and December 2007. All patients were treated on an inpatient basis. In every case, CEUS was carried out the day before RFA. Detection of HCC nodules was compared between CEUS and conventional US, using dynamic CT as the reference standard. In 291 patients, CEUS was carried out also during RFA. We assessed whether CEUS facilitated RFA by comparing the numbers of RFA sessions per treatment in CEUS-assisted RFA and in historical controls matched for tumor and background conditions, performed with conventional US between January 2004 and July 2007. The study protocol conformed to the ethical guidelines of the Helsinki Declaration 2004 and was approved by the research ethics committee of the authors' institution.

Diagnosis of HCC

HCC was diagnosed by dynamic CT, considering hyperattenuation in the arterial phase with washout in the late phase as a definite finding.[16] Multidetector-row CT (MDCT) was performed within a month before RFA, where plain and dynamic contrast-enhanced CT images were obtained with rapid intravenous injection of a contrast material. MDCT systems used for our study were Aquillion 64 (Toshiba, Tokyo, Japan) or LightSpeed VCT (GE Healthcare, Milwaukee, WI, USA). A bolus of iodinated contrast material was injected using a mechanical power injector in 30 s, at a concentration of 300–370 mg I/mL for the amount of bodyweight (kg) × 2 mL (maximum, 100 mL). The three contrast-enhanced phases (early arterial phase, late arterial phase, and equilibrium phase) were obtained at 25, 40, and 120 s after the start of injection. Reconstruction images were obtained with a section thickness of 2.5 mm with a reconstruction interval of 1.5 mm. Most HCC nodules were also confirmed histopathologically with ultrasound-guided biopsy afterwards. The pathological grade was evaluated based on Edmondson–Steiner criteria.[17]

Ultrasound examinations

All US examinations were carried out using the SSA-770A apparatus (APLIO; Toshiba, Tokyo, Japan), on patients after at least 5 h of fasting. First, we examined the liver for HCC lesions with conventional tissue harmonic imaging. We performed both intercostal and subcostal scans of the right lobe, and both sagittal and transverse scans of the left lobe. Efforts were exerted to maximize visualization of lesions, including positional changes and breath holding. Then, CEUS was performed by the same operator with phase inversion mode imaging. A 0.5-mL dose of Sonazoid was injected into an antebrachial vein at 0.2 mL/s via a 21-gauge cannula, followed by 20-mL of normal saline. The whole liver was scanned with CEUS, using similar techniques as used in the conventional US, 10 min after Sonazoid injection. When visualization was not sufficient at that time, a CEUS scan was repeated after a 5–10-min interval. Findings in conventional US and CEUS were separately recorded by the operator. Detection ability of US and CEUS was calculated using dynamic CT as a reference standard. We analyzed the correlation between the number of additionally detected nodules by CEUS and liver function reservoir, as represented by serum albumin concentration.

RFA sessions

Inclusion criteria for percutaneous ablation were as follows: total bilirubin concentration lower than 3 mg/dL; platelet count not less than $50 \times 10^3/mm^3$; and prothrombin activity not lower than 50%. Patients with portal vein tumor thrombosis, refractory ascites, or extrahepatic metastasis were excluded. The procedure has been meticulously described elsewhere.[18] In brief, grounding was achieved by attaching two pads to the patient's thighs. A 17-gauge, cooled-tip electrode with a 2- or 3-cm exposed tip was attached to a radiofrequency generator (Covidien, Mansfield, MA, USA). After local anesthesia, the electrode was inserted under ultrasound guidance. During ablation, the temperature was measured with a thermocouple in the electrode and tissue impedance was also monitored by a circuitry incorporated into the generator. A peristaltic pump infused 0°C saline into the electrode lumen to maintain the tip temperature below 20°C. Radiofrequency energy was delivered for 6–12 min on each application. A 12-min ablation using a 3-cm electrode would produce a quasi-spherical necrotic volume 3 cm in diameter. For larger lesions, the electrode was repeatedly inserted into different sites, so that the entire lesion could be enveloped by assumed necrotic volumes.

CEUS-assisted RFA was done basically with Kupffer imaging at least 10 min after Sonazoid injection. Electrodes were inserted after perfluorobutane microbubbles disappeared from vessels so that the vessels were well visualized. Before the introduction of CEUS, when a nodule was not well visualized by conventional US, the needle was inserted by real-time ultrasound reference to the portal vein or hepatic vein near the target nodule.

The efficacy of RFA was assessed with contrast-enhanced CT performed on the next day. Complete ablation was defined as hypoattenuation of each lesion with a sufficient safety margin in the surrounding liver parenchyma. When ablation was found to be insufficient, an additional session of RFA was carried out, until complete ablation was confirmed on contrast-enhanced CT. The number of RFA sessions was defined as the total number of intervention episodes required to achieve complete ablation.

Follow up

Each patient was followed up with contrast-enhanced CT every 4 months. Tumor recurrence was diagnosed according to the

© 2011 Journal of Gastroenterology and Hepatology Foundation and Blackwell Publishing Asia Pty Ltd

same criteria applied to initial HCC diagnosis. Intrahepatic recurrence was classified as either recurrence at a site distant from the primary site or that adjacent to the treated lesion (local tumor progression).

Historical controls

One historical control was selected for each patient who underwent CEUS-assisted RFA from patients who received RFA between January 2004 and July 2007, that is, prior to the introduction of CEUS ($n = 2261$). The maximum diameter of tumors (± 0.3 cm), the number of lesions (exact), viral markers (exact), and serum albumin concentration (± 0.3 g/dL) were used as the matching factors, with the maximum permissible differences shown in parentheses. The selection was carried out using the find-matches function of S-Plus 2000 (TIBCO Software, Palo Alto, CA, USA).

Statistical analysis

Variables were expressed as mean ± standard deviation unless otherwise specified. Continuous variables were compared using the unpaired Student's *t*-test, and categorical variables were compared using Fisher's exact probability test. The number of RFA sessions per patient was compared using the Mann–Whitney *U*-test. All tests were two-sided with a significance level of 5%. Statistical analyses were carried out with S-plus 2000.

Results

The baseline characteristics of patients who underwent CEUS are shown in Table 1. The patients consisted of 216 men and 100 women with a mean age of 70.1 ± 7.7 years. The mean maximum diameter of tumors was 1.6 ± 0.8 cm. All 316 patients underwent both conventional US and CEUS, in this order, the day before scheduled RFA. Of 716 HCC nodules diagnosed on dynamic CT, conventional US identified 598 (83.5%) nodules as definite lesions. Subsequent CEUS detected an additional 69 nodules, increasing the detectability to 93.2%, and the difference was statistically significant ($P = 0.04$). The number of additionally detected nodules per patient was one in 36 patients, two in eight, three in five, and more than three in three; thus at least one nodule was additionally detected with CEUS in a total of 52 patients (16.5%). Among these patients, artificial pleural effusion was used in 19 cases and artificial ascites was used in four patients, resulting in additional detection of 28 and four nodules, respectively. The number of additionally detected nodules by CEUS was positively correlated with serum albumin concentration ($P = 0.016$) (Fig. 1).

CEUS was also used during the RFA session in 291 patients. Artificial pleural effusion was performed in 71 (24.4%) cases and artificial ascites was used in 27 (9.1%) cases. Two demonstrative cases successfully treated with CEUS-assisted RFA are shown in Figures 2 and 3. We did not conduct randomization on the use of CEUS because its usefulness in tumor visualization was obvious at least in a proportion of the patients. Instead, we chose historical controls matched for tumor-related factors and liver function, and compared the number of RFA sessions per patient and total ablation time per session. In all patients including controls, RFA sessions were repeated until complete ablation of each nodule was confirmed on contrast-enhanced CT. The mean number of RFA sessions per patient was 1.33 ± 0.45 in patients with CEUS, as compared to 1.49 ± 0.76 in the historical controls ($P = 0.0019$ by Mann–Whitney *U*-test) (Table 2). Total ablation time per session was 17.2 ± 10.7 min with CEUS-assisted RFA and 15.7 ± 9.6 min in the historical controls ($P = 0.156$ by Mann–Whitney *U*-test). Treatment-related complications occurred in six patients (1.9%) who received CEUS-assisted RFA: peritoneal bleeding in three patients and hemothorax, bile duct bleeding, and dermal burn each in one patient. There was no treatment-related death. The incidence of complications did not differ in the historical controls (1.7%, $P = 0.867$ by Fisher's exact probability test). During the follow up, local tumor progression was detected in six patients (2.1%) who received CEUS-assisted RFA and in eight

Table 1 Baseline characteristics ($n = 316$)

Variables	
Age (years)†	70.1 ± 7.7
Male, *n* (%)	216 (68.3)
HBsAg positive, *n* (%)	45 (14.2)
HCVAb positive, *n* (%)	238 (75.3)
Diameter (cm)†	1.6 ± 0.8
Number of tumors	
1, *n* (%)	124 (39.3)
2–3, *n* (%)	143 (45.2)
≥ 4, *n* (%)	49 (15.5)
Total bilirubin (mg/dL)‡	0.9 (0.6–1.2)
Albumin (g/dL)‡	3.6 (3.2–3.9)
Platelet count (10^4/mm^3)‡	10.5 (7.3–13.8)
AFP (ng/mL)‡	16.9 (6.0–62.8)
L3 (%)‡	0.5 (0–3.1)
DCP (mAU/mL)‡	20 (13–50)

†Mean ± standard deviation.
‡Median (25th–75th percentiles).
AFP, alpha-fetoprotein; DCP, des-gamma-carboxy-prothrombin; HBsAg, hepatitis B surface antigen; HCVAb, hepatitis C virus antibody.

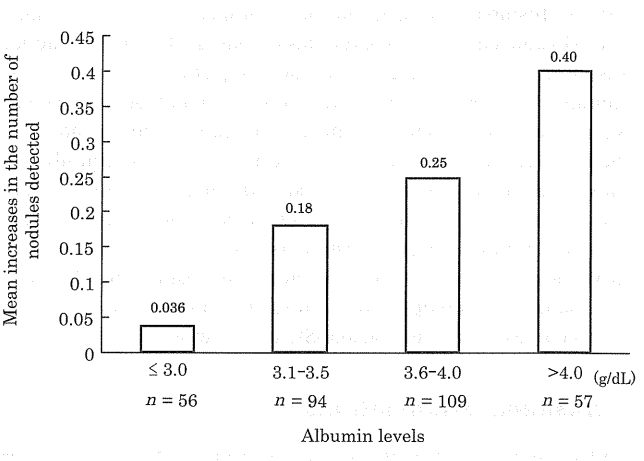

Figure 1 The mean increases in detected tumor number with contrast-enhanced ultrasonography were well correlated with serum albumin level ($P = 0.016$).

© 2011 Journal of Gastroenterology and Hepatology Foundation and Blackwell Publishing Asia Pty Ltd

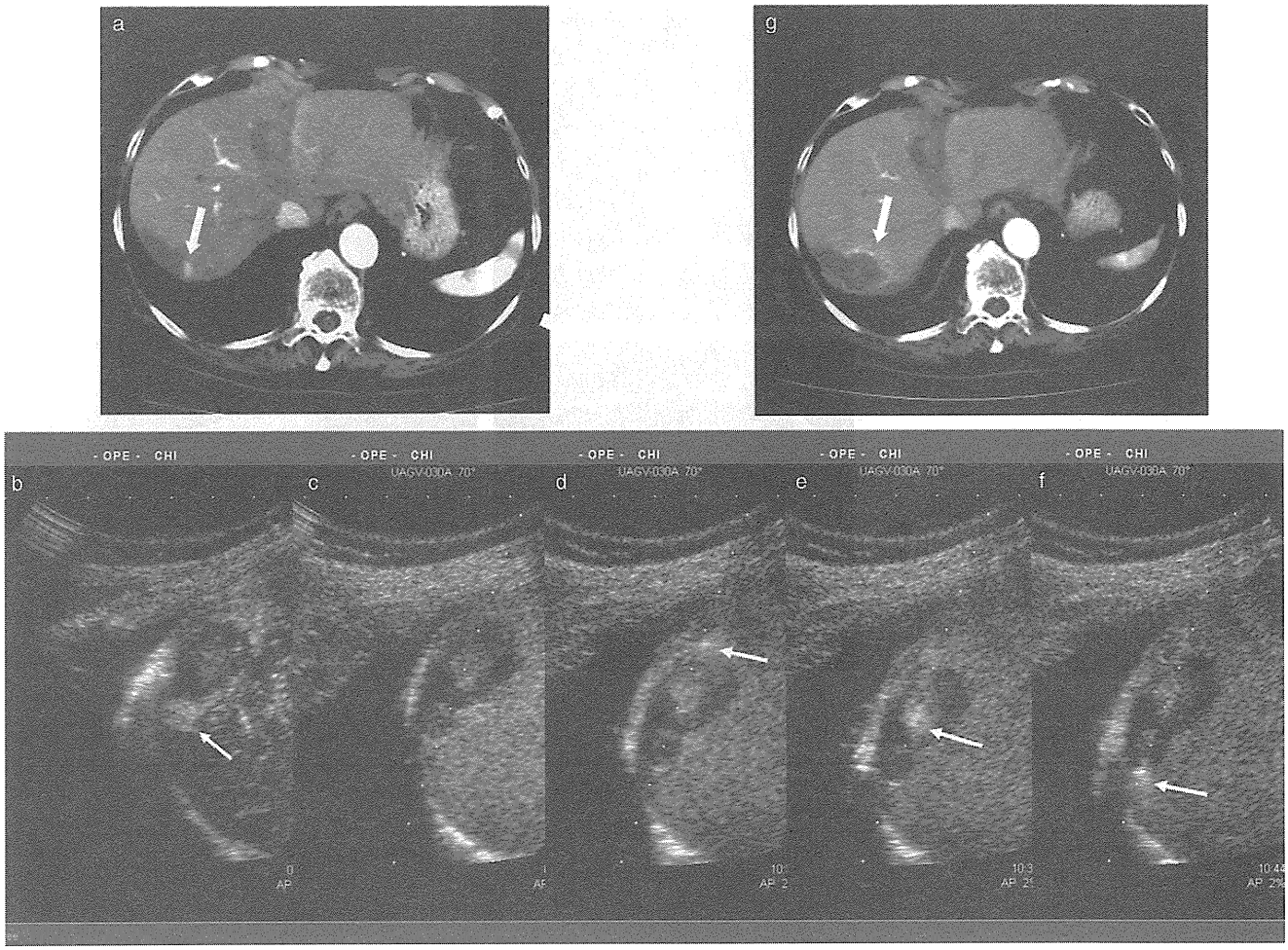

Figure 2 (a) An 80-year-old woman with hepatocellular carcinoma. Computed tomography (CT) revealed a nodule with hyperattenuation in the early arterial phase near a previously ablated lesion. (b) After injection of Sonazoid with artificial right pleural effusion, the nodule was clearly detected as a hyperechoic lesion (arrows). (c–f) Radiofrequency ablation of the nodule. (Arrows indicate the tip of radiofrequency needle). (g) Evaluation CT confirmed that the nodule was sufficiently ablated.

historical controls (2.7%, $P = 0.788$ by Fisher's exact probability test).

Discussion

In the present study, we have shown that the number of RFA sessions required per patient was significantly decreased when using the new US contrast agent, Sonazoid, as compared to historical controls. These were accomplished without increasing the incidence of local tumor progression or treatment-related complications. At the authors' institution, RFA is repeated until complete ablation of each HCC nodule is confirmed by dynamic CT. Without CEUS, when the tumor was not well delineated on conventional US, ablation used to be performed based on the information on CT and indecisive US images, which may have led to insufficient ablation revealed by evaluation CT, requiring an additional ablation session. Thus it can be assumed that the decreased number of RFA sessions with Sonazoid is mainly due to improvement in tumor detection and delineation. Unnecessary ablation of non-cancerous liver parenchyma may have deleterious effects on liver function and may reduce survival time. Thus the decrease in the number of RFA sessions is beneficial not only in cost reduction but possibly also for patients' survival.

The detectability of HCC nodules was increased from 83.5% to 93.2% with the use of CEUS, as determined with contrast CT as the reference standard. The benefit of using Sonazoid to detect "invisible" nodules by conventional US was more apparent in those with higher serum albumin concentration, suggesting that the resolution of Sonazoid CEUS may be compromised when liver function is substantially impaired. Uptake of perfluorobutane in non-cancerous liver depends on Kupffer cell function, which may be severely impaired in advanced liver diseases. A similar phenomenon was also reported in super paramagnetic iron oxide (SPIO)-enhanced magnetic resonance imaging.[19] Thus the contrast between HCC and non-cancerous parenchyma in Kupffer imaging can be diminished when liver function reservoir is poor. In the present study we obtained Kupffer imaging up to 30 min after

© 2011 Journal of Gastroenterology and Hepatology Foundation and Blackwell Publishing Asia Pty Ltd

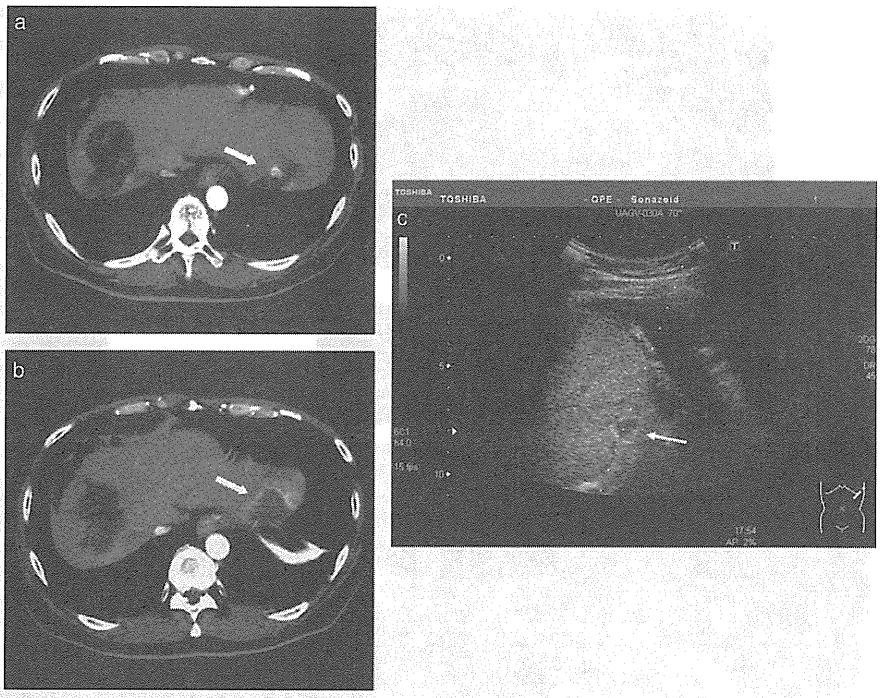

Figure 3 (a) A 52-year-old man with hepatocellular carcinoma. Computed tomography revealed a nodule at the left lateral lobe. (b) This lesion was clearly detected as an enhanced defect in the Kupffer imaging phase. Artificial left pleural effusion was used. (c) The nodule was sufficiently ablated.

Table 2 Comparison of the number of sessions

Variables	Contrast-enhanced ultrasonography group ($n = 291$)	Historical control group ($n = 291$)	*P* value
Maximum diameter (cm)†	1.9 ± 0.8	1.9 ± 0.8	0.94
Number of tumors†	2.1 ± 1.3	2.1 ± 1.3	1.00
Albumin‡	3.5 (3.2–3.9)	3.5 (3.2–3.9)	0.94
Platelet count‡	10.3 (7.8–11.5)	10.5 (7.3–11.3)	0.67
Ablation time per session (min)†	17.2 ± 10.7	15.7 ± 9.6	0.156
Mean number of sessions†	1.33 ± 0.45	1.49 ± 0.76	0.0019

†Mean ± standard deviation.
‡Median (25th–75th percentiles).

Sonazoid injection in cases of insufficient visualization of lesions. Uptake of perfluorobutane in liver parenchyma might have been increased with longer intervals. However, the appropriate interval for observing Kupffer imaging relative to the level of liver function level is not known. Thus, the possibility of detection failure with Sonazoid CEUS should be noted, especially in cases of advanced liver dysfunction.

During the present study, we noticed other limitations of CEUS with Sonazoid. As with conventional US, nodules in certain locations of the liver, such as those immediately below the diaphragm, are difficult to visualize clearly enough for safe and effective RFA even with Sonazoid. For such nodules, the artificial pleural effusion may be useful.[20] Artificial ascites may be useful for the demarcation of nodules near the gastrointestinal tract.[21] Indeed, in the present study, artificial pleural effusion was used in 24.4% of cases and artificial ascites was used in 9.1%, resulting in additional detection of 28 and four nodules, respectively. These techniques are useful in visualizing nodules at certain locations and may enhance the usability of CEUS.

The present study was not a randomized controlled trial directly comparing CEUS with Sonazoid and conventional US, but an analysis of utility of CEUS in RFA, which was analyzed by using historical matched controls. This study design was a compromise with the fact that the final diagnosis was based on dynamic CT, and it was unethical not to use CEUS in case of discrepancy between conventional US and dynamic CT. The historical controls were selected from HCC patients who were treated with RFA after 2004. Since that period, we have performed RFA with the same CT and US apparatuses. Precise comparison of the detection ability and resolution of HCC nodules between conventional US and CEUS will require studies with a design different from the present one.

In conclusion, CEUS with Sonazoid is useful in visualizing HCC nodules that are difficult to detect with conventional US. The number of RFA sessions required for complete ablation of every nodule was decreased in CEUS-assisted RFA, indicating that Sonazoid is a useful supportive agent in RFA. However, the effectiveness of Sonazoid may be compromised in case of severe liver dysfunction.

© 2011 Journal of Gastroenterology and Hepatology Foundation and Blackwell Publishing Asia Pty Ltd

References

1 Parkin DM, Bray F, Ferlay J, Pisani P. Global cancer statistics, 2002. *CA Cancer J. Clin.* 2005; **55**: 74–108.
2 Bruix J, Sherman M. Management of hepatocellular carcinoma. *Hepatology* 2005; **42**: 1208–36.
3 Rossi S, Di Stasi M, Buscarini E *et al.* Percutaneous RF interstitial thermal ablation in the treatment of hepatic cancer. *AJR Am. J. Roentgenol.* 1996; **167**: 759–68.
4 Livraghi T, Goldberg SN, Lazzaroni S, Meloni F, Solbiati L, Gazelle GS. Small hepatocellular carcinoma: treatment with radio-frequency ablation versus ethanol injection. *Radiology* 1999; **210**: 655–61.
5 Shiina S, Teratani T, Obi S *et al.* A randomized controlled trial of radiofrequency ablation with ethanol injection for small hepatocellular carcinoma. *Gastroenterology* 2005; **129**: 122–30.
6 Ikai I, Arii S, Okazaki M *et al.* Report of the 17th nationwide follow-up survey of primary liver cancer in Japan. *Hepatol. Res.* 2007; **37**: 676–91.
7 Tanaka S, Kitamura T, Nakanishi K, Okuda S, Kojima J, Fujimoto I. Recent advances in ultrasonographic diagnosis of hepatocellular carcinoma. *Cancer* 1989; **63**: 1313–7.
8 Nakai M, Sato M, Sahara S *et al.* Radiofrequency ablation assisted by real-time virtual sonography and CT for hepatocellular carcinoma undetectable by conventional sonography. *Cardiovasc Intervent Radiol.* 2009; **32**: 62–9.
9 Sato M, Watanabe Y, Tokui K, Kawachi K, Sugata S, Ikezoe JC. T-guided treatment of ultrasonically invisible hepatocellular carcinoma. *Am. J. Gastroenterol.* 2000; **95**: 2102–6.
10 Fujimoto M, Moriyasu F, Nishikawa K, Nada T, Okuma M. Color Doppler sonography of hepatic tumors with a galactose-based contrast agent: correlation with angiographic findings. *AJR Am. J. Roentgenol.* 1994; **163**: 1099–104.
11 Kudo M, Tomita S, Tochio H *et al.* Sonography with intraarterial infusion of carbon dioxide microbubbles (sonographic angiography): value in differential diagnosis of hepatic tumors. *AJR Am. J. Roentgenol.* 1992; **158**: 65–74.
12 Kudo M. New sonographic techniques for the diagnosis and treatment of hepatocellular carcinoma. *Hepatol. Res.* 2007; **37** (Suppl. 2): S193–9.
13 Moriyasu F, Itoh K. Efficacy of perflubutane microbubble-enhanced ultrasound in the characterization and detection of focal liver lesions: phase 3 multicenter clinical trial. *AJR Am. J. Roentgenol.* 2009; **193**: 86–95.
14 Numata K, Morimoto M, Ogura T *et al.* Ablation therapy guided by contrast-enhanced sonography with Sonazoid for hepatocellular carcinoma lesions not detected by conventional sonography. *J. Ultrasound Med.* 2008; **27**: 395–406.
15 Minami Y, Kudo M, Hatanaka K *et al.* Radiofrequency ablation guided by contrast harmonic sonography using perfluorocarbon microbubbles (Sonazoid) for hepatic malignancies: an initial experience. *Liver Int.* 2010; **30**: 759–64.
16 Torzilli G, Minagawa M, Takayama T *et al.* Accurate preoperative evaluation of liver mass lesions without fine-needle biopsy. *Hepatology* 1999; **30**: 889–93.
17 Edmondson HA, Steiner PE. Primary carcinoma of the liver: a study of 100 cases among 48 900 necropsies. *Cancer* 1954; **7**: 462–503.
18 Tateishi R, Shiina S, Teratani T *et al.* Percutaneous radiofrequency ablation for hepatocellular carcinoma. An analysis of 1000 cases. *Cancer* 2005; **103**: 1201–9.
19 Tanimoto A, Yuasa Y, Shinmoto H *et al.* Superparamagnetic iron oxide-mediated hepatic signal intensity change in patients with and without cirrhosis: pulse sequence effects and Kupffer cell function. *Radiology* 2002; **222**: 661–6.
20 Kondo Y, Yoshida H, Tateishi R, Shiina S, Kawabe T, Omata M. Percutaneous radiofrequency ablation of liver cancer in the hepatic dome using the intrapleural fluid infusion technique. *Br. J. Surg.* 2008; **95**: 996–1004.
21 Kondo Y, Yoshida H, Shiina S, Tateishi R, Teratani T, Omata M. Artificial ascites technique for percutaneous radiofrequency ablation of liver cancer adjacent to the gastrointestinal tract. *Br. J. Surg.* 2006; **93**: 1277–82.

© 2011 Journal of Gastroenterology and Hepatology Foundation and Blackwell Publishing Asia Pty Ltd

Research Article

EASL EUROPEAN ASSOCIATION FOR THE STUDY OF THE LIVER | JOURNAL OF HEPATOLOGY

Pathogenesis of lipid metabolism disorder in hepatitis C: Polyunsaturated fatty acids counteract lipid alterations induced by the core protein

Hideyuki Miyoshi[1], Kyoji Moriya[1], Takeya Tsutsumi[1], Seiko Shinzawa[1], Hajime Fujie[1], Yoshizumi Shintani[1], Hidetake Fujinaga[1], Koji Goto[1], Toru Todoroki[2], Tetsuro Suzuki[3], Tatsuo Miyamura[3], Yoshiharu Matsuura[4], Hiroshi Yotsuyanagi[1], Kazuhiko Koike[1,*]

[1]*Department of Internal Medicine, Graduate School of Medicine, University of Tokyo, Tokyo, Japan;* [2]*Department of Laboratory Medicine, Keio University School of Medicine, Tokyo, Japan;* [3]*Department of Virology II, National Institute of Infectious Diseases, Tokyo, Japan;* [4]*Department of Molecular Virology, Research Institute for Microbial Diseases, Osaka University, Osaka, Japan*

Background & Aims: Disturbance in lipid metabolism is one of the features of chronic hepatitis C, being a crucial determinant of the progression of liver fibrosis. Experimental studies have revealed that the core protein of hepatitis C virus (HCV) induces steatosis.

Methods: The activities of fatty acid metabolizing enzymes were determined by analyzing the fatty acid compositions in HepG2 cells with or without core protein expression.

Results: There was a marked accumulation of triglycerides in core-expressing HepG2 cells. While the oleic/stearic acid (18:1/18:0) and palmitoleic/palmitic acid ratio (16:1/16:0) were comparable in both the core-expressing and the control cells, there was a marked accumulation of downstream product, 5,8,11-eicosatrienoic acid (20:3(n-9)) in the core-expressing HepG2 cells. The addition of eicosatetraynoic acid, which inhibits delta-6 desaturase activity which is inherently high in HepG2 cells, led to a marked accumulation of oleic and palmitoleic acids in the core-expressing cells, showing that delta-9 desaturase was activated by the core protein. Eicosapentaenoic acid (20:5(n-3)) or arachidonic acid (20:4(n-6)) administration significantly decreased delta-9 desaturase activity, the concentration of 20:3(n-9), and triglyceride accumulation. This lipid metabolism disorder was associated with NADH accumulation due to mitochondrial dysfunction, and was reversed by the addition of pyruvate through NADH utilization.

Conclusions: The fatty acid enzyme, delta-9 desaturase, was activated by HCV core protein and polyunsaturated fatty acids counteracted this impact of the core protein on lipid metabolism. These results may open up new insights into the mechanism of lipid metabolism disorder associated with HCV infection and provide clues for the development of new therapeutic devices.

© 2010 European Association for the Study of the Liver. Published by Elsevier B.V. All rights reserved.

Keywords: Steatosis; Oleic acid; Core protein; Lipid metabolism; Desaturase; Hepatocellular carcinoma; NADH.

Received 31 March 2010; received in revised form 8 June 2010; accepted 5 July 2010; available online 22 September 2010

* Corresponding author. Address: Department of Gastroenterology, Graduate School of Medicine, University of Tokyo, 7-3-1 Hongo, Bunkyo-ku, Tokyo 113-8655, Japan. Tel.: +81 3 5800 8800; fax: +81 3 5800 8799.

E-mail address: kkoike-tky@umin.ac.jp (K. Koike).

Abbreviations: HCV, hepatitis C virus; HCC, hepatocellular carcinoma; PUFA, polyunsaturated fatty acids; PPAR, peroxisome proliferators-activated receptors; SREBP, sterol regulatory element binding protein; EPA, eicosapentaenoic acid; AA, arachidonic acid; ETYA, eicosatetraynoic acid; NADH, nicotinamide adenine dinucleotide; KBR, ketone body ratio.

Introduction

Persistent hepatitis C virus (HCV) infection leads to the development of chronic hepatitis, cirrhosis, and eventually, hepatocellular carcinoma (HCC), thereby being a serious problem worldwide both in medical and in socio-economical settings [1]. Histologically, several distinct features, such as bile duct damage, lymphoid follicle formation, and steatosis, (fatty change) characterize chronic hepatitis C [2–4]. Among these, steatosis is reproducible in experimental systems, both *in vitro* and *in vivo*, in which HCV proteins, particularly the core protein of HCV, are expressed. The introduced core gene induces the formation of lipid droplets in the cytoplasm of cultured cells [5,6], and in transgenic mice, it induces hepatic steatosis resembling that in chronic hepatitis C patients [7–10].

In addition, evidence has accumulated showing that steatosis is a crucial determining factor for the progression of liver fibrosis [11–13]. Steatosis and serum lipid profiles are also associated with sustained virological response to ribavirin/interferon combination therapy [14,15]. Moreover, HCV transgenic mice resemble chronic hepatitis C patients in terms of the development of HCC, implying that the HCV core protein is one of the most important viral molecules in the pathogenesis of hepatitis C [16,17]. It would thus be meaningful to explore the precise role of the core protein in modulating lipid metabolism, which may also be involved in hepatocarcinogenesis. More recently, involvement of the metabolism of lipids such as sphingolipids or cholesterol has been implicated in the replication of HCV, with a formation of lipid rafts, which are considered to be the place for HCV replication [18,19], hereby highlighting again the importance of lipid metabolism in HCV infection.

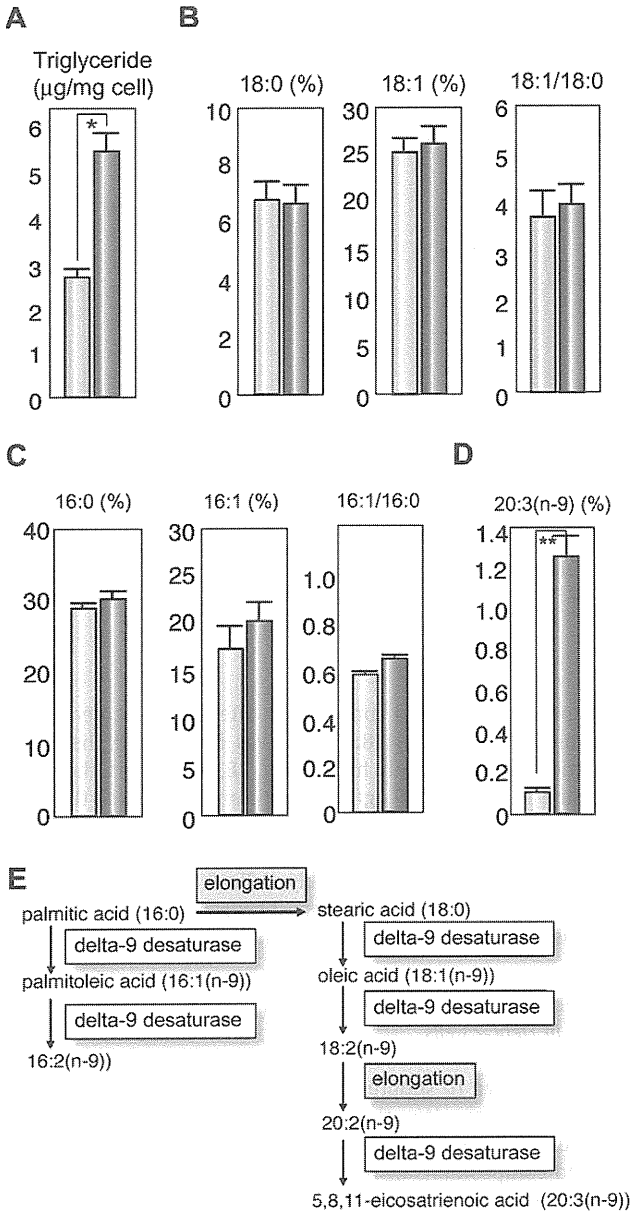

Fig. 1. Effect of the core protein on fatty acid composition in HepG2 cells. The fatty acid compositions of the total cell lipids were analyzed and the ratios of 18:1/18:0 and 16:1/16:0 in the core-expressing and control HepG2 cells were calculated. (A) Concentrations of triglycerides. (B) Percentages of stearic acid (18:0) and oleic acid (18:1(n-9)), and the 18:1/18:0 ratio. (C) Percentages of palmitic acid (16:0) and palmitoleic acid (16:1(n-9)), and the 16:1/16:0 ratio. (D) Percentage of eicosatrienoic acid (20:3(n-9). (E) Schematic display of synthetic pathway of n-9 fatty acids. Light blue bars indicate control cells and dark blue bars indicate core-expressing cells. Values represent the mean ± SE, $n = 5$ in each group. $^{*}p < 0.05$, $^{**}p < 0.01$.

Previously, we reported that the concentration of oleic acid (18:1(n-9)) was increased compared with that of stearic acid (18:0) in liver tissues of chronic hepatitis C patients as well as in those of mice transgenic for the HCV core gene [8]. Such a change may lead to increased membrane fluidity, owing to the lower melting temperature of monounsaturated fatty acids, resulting in incremental metabolism and proliferation of hepatocytes [20–22]. On the other hand, polyunsaturated fatty acids (PUFAs), such as eicosapentaenoic acid (20:5(n-3)) and arachidonic acid (20:4(n-6)), are known to activate the nuclear transcription of peroxisome proliferator-activated receptors (PPAR) and suppress the sterol regulatory element binding protein (SREBP)-1. While PPARγ induces delta-9 desaturase (stearoyl-CoA desaturase) gene expression, PUFAs suppresses delta-9 desaturase activity [23]. In the current study, we determined fatty acid desaturase activities by analyzing the fatty acid compositions in HepG2 cells expressing HCV core protein by chromatography. In addition, we determined whether exogenous PUFAs restore HCV-associated changes in fatty acid metabolism.

Materials and methods

Reagents

Eicosapentaenoic acid (EPA), arachidonic acid (AA), and eicosatetraynoic acid (ETYA) were purchased from Sigma Chemical (St. Louis, MO). Other chemicals were of analytical grade and purchased from Wako Chemicals (Tokyo, Japan).

Cell culture

This study was performed using HepG2 cell lines expressing the HCV core protein under the control of the CAG promoter (Hep39J, Hep396 and Hep397), or a control HepG2 line (Hepswx) carrying an empty vector, which were described previously [24], and control bulk HepG2 cells. They were maintained in Dulbecco's modified Eagle's medium (DMEM), supplemented with 10% fetal bovine serum (Invitrogen), 1 mg/ml G418, 100 U/ml penicillin, and 100 μg/ml streptomycin in a humidified atmosphere at 37 °C in 5% CO_2. Fatty acids were dissolved in DMEM containing defatted bovine serum albumin. The ratio of fatty acids to albumin (mole/mole) was 0.7. The cells were exposed to fatty acid–albumin complexes at various concentrations for 48 h. All the experiments were repeated at least five times.

Lipid extraction, measurement of triglyceride content, and analysis of fatty acid composition

Total cell lipids were extracted by Foch's method. The cells were washed twice with phosphate-buffered saline and collected by centrifugation. The cell pellets were homogenized with 10 vole of chloroform: methanol solution (2:1), and the mixture was shaken for 5 min. The lower phase was then washed with 4 vole of saline, dried on anhydrous sodium sulfate, and evaporated to complete dryness. For the analysis of fatty acid composition, the residue was methanolysed by the modified Morrison and Smith method with boron trifluoride as a catalyst [25]. Fatty acid methyl esters were analyzed using a Shimadzu GC-7A gas chromatograph (Shimadzu Corp., Kyoto, Japan).

Measurement of the ketone body ratio and lactate/pyruvate

The cells were cultured to confluence on 3.5 cm dishes, and the medium was replaced with 700 μl of fresh one. After 24 h of incubation, the levels of acetoacetate and β-hydroxybutyrate in the medium were measured by monitoring the production or consumption of nicotinamide adenine dinucleotide (NADH) with Ketorex kit (Sanwa Chemical, Nagoya, Japan) [26]. The ketone body ratio (KBR) was calculated as the acetoacetate/β-hydroxybutyrate ratio. The lactate and pyruvate levels in the medium were measured at random times by the lactate oxidase method and pyruvate oxidase method, respectively.

Effect of pyruvate on lipid metabolism

In some experiments, pyruvate (Wako Chemicals) was added to culture medium at a final concentration of 0, 1, 5, or 10 mM. After 48 h of incubation at 37 °C, the cells were harvested and subjected to fatty acid composition analysis or real-time PCR analysis.

Real-time PCR

RNA was prepared from cultured cells using TRIzol LS (Invitrogen, Carlsbad, CA). The fluorescent signal was measured using ABI prism 7000 (Applied Biosystems, Tokyo, Japan). The genes encoding mouse sterol regulatory element-binding proteins (SREBP)-1a, SREBP-1c, delta-9 desaturase, and hypoxanthine phosphoribosyltransferase were amplified with the primer pairs CACAGCGGTTTTGAACGAC and CTGGCTCCTCTTTGATCCCA, ACGGAGCCATGGATTGCACATTTG and TACATCTT TAAAGCAGCGGGTGCCGATGGT, TTCCCTCCTGCAAGCTCTAC and CGCAAGAAGG TGCTAACGAAC, and CCAGCAAGCTTGCAACCTTAACCA and GTAATGATCAGTCAAC GGGGGAC, respectively.

Statistical analysis

Data are presented as the mean ± SE. The data were analyzed by Mann–Whitney *U* test. Differences were considered statistically significant when $p < 0.05$.

Results

Triglyceride content in HepG2 cells expressing HCV core protein

To validate the relationship between the lipid accumulation and the core protein, we first determined the triglyceride contents in core-protein-expressing HepG2 clones (core-expressing cells), Hep39J, Hep396, Hep397, and control HepG2 cells. Core-expressing Hep396 cells contained significantly larger amounts of triglyceride than the control cells (Fig. 1A, $p < 0.01$), which are consistent with the results of previous studies on culture cells and transgenic mice [6,7,27]. Similar results were obtained with the other core-expressing cell lines.

Fatty acid compositions of total cell lipids

Analysis on the fatty acid compositions of total lipids revealed that the concentration of oleic acid (18:1(n-9)) and the ratio of oleic acid/stearic acid (18:1/18:0) in the core-expressing cells are similar to those in the control cells (Fig. 1B). The ratio of palmitoleic acid (16:1(n-9))/palmitic acid (16:1/16:0) was higher in the core-expressing cells than that in the control cells, but the difference was not significant (Fig. 1C). This rather dissociates from the results obtained in HCV core gene transgenic mice, in which the 18:1/18:0 ratio was significantly higher than that in control mice, thereby suggesting an increased delta-9 desaturase activity as a consequence of the HCV core protein expression [8]. However, it should be noted that the concentration of 5,8,11-eicosatrienoic acid (20:3(n-9)), a downstream product of n-9 fatty acid desaturation, was approximately13 times higher in the core-expressing cells than that in the control cells (Fig. 1D and E, $p < 0.01$). This is due to the fact that the activity of the delta-6 desaturase, an enzyme downstream of delta-9 desaturase, is also high in HepG2 cells, resulting in the relatively lower concentration of 18:1 in the core-expressing cells despite the high delta-9 desaturase activity. Actually, the delta-6 desaturase activity has been shown to be inherently high in HepG2 cells [28,29].

To verify this possibility, we administered ETYA, which inhibits delta-6 desaturase activity, to the cell cultures. Because similar results were obtained with the other core-expressing HepG2 cell lines, subsequent experiments were carried out using the Hep396 cell line. The addition caused significant increases in both 18:1/18:0 and 16:1/16:0 ratios in the core-expressing cells but not in the control cells (Fig. 2A 0 vs. 10 μg/ml and 0 vs. 50 μg/ml; $p < 0.05$, respectively). When compared between the

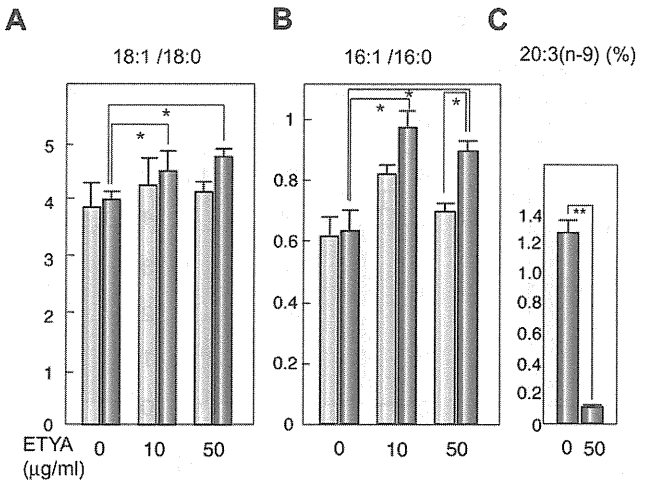

Fig. 2. Effect of ETYA on delta-9 desaturase index. HepG2 cells with or without the core protein were incubated with ETYA for 48 h. The fatty acid compositions of the total cell lipids were analyzed, and the ratios of 18:1/18:0 (A) and 16:1/16:0 (B), and the percentage of eicosatrienoic acid (20:3(n-9) (C) were computed. Light blue bars indicate control cells and dark blue bars indicate core-expressing cells. $N = 5$ in each group. $^*p < 0.05$. ETYA, eicosatetraynoic acid.

core-expressing cells and control cells after the treatment with 50 μg/ml ETYA, the 18:1/18:0 ratio was higher and the 16:1/16:0 ratio was significantly higher (Fig. 2B, $p < 0.05$) in the core-expressing cells. ETYA (50 μg/ml) significantly decreased the concentration of 20:3(n-9) in the core-expressing cells (Fig. 2C, $p < 0.01$). These results suggest that the HCV core protein enhances the activities of delta-9, and possibly, delta-5 desaturases, modulating fatty acid metabolism in HepG2 cells, in which the delta-6 desaturase activity is intrinsically high (Fig. 1E) [28,29].

PUFAs modify fatty acid compositions and decrease triglyceride contents in HepG2 Cells

PUFAs are known to suppress the activities of both delta-9 and delta-6 desaturases. We, therefore, added PUFA, EPA, or AA, to the culture cell medium to examine the effect of PUFAs on the fatty acid compositions in HepG2 cells expressing the core protein. EPA and AA individually decreased the 18:1/18:0 and 16:1/16:0 ratios in a similar extent in both the core-expressing cells and the control cells (Fig. 3, $p < 0.05$). EPA and AA also significantly decreased the concentration of 20:3(n-9) in the core-expressing cells in a dose-dependent manner (Fig. 4, $p < 0.05$). In addition, EPA and AA individually decreased the triglyceride concentration in cells, in particular, in the core-expressing cells (Fig. 5, in core-expressing cells, $p < 0.01$; in control cells, $p < 0.05$, respectively).

Ketone body ratio and lactate/pyruvate ratio

Although the mechanism by which the HCV core protein enhances fatty acid desaturation is yet unclear, one possibility is the creation of an overreduced state in the core-expressing cells. The overreduced state or the accumulation of NADH in cells is known to accelerate the activities of fatty acid desaturases [30,31]. Such a condition may originate from the dysfunction of the mitochondrial electron transfer system (ETS), which has been

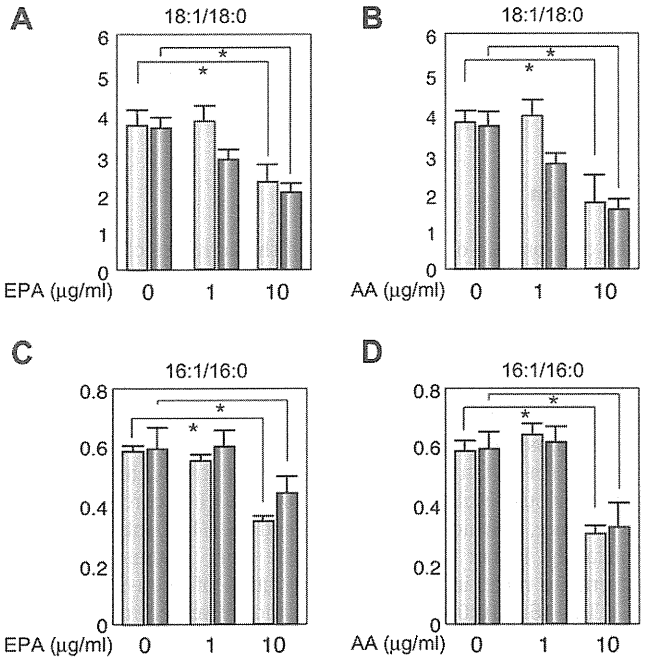

Fig. 3. Effect of EPA and AA on delta-9 desaturase index. HepG2 cells with or without the core protein were incubated with EPA (A and C) or AA (B and D) for 48 h. The fatty acid compositions of the total cell lipids were analyzed and the ratios of 18:1/18:0 (A and B) and 16:1/16:0 (C and D) were computed. Light blue bars indicate control cells and dark blue bars indicate core-expressing cells. $N = 5$ in each group. $^{*}p < 0.05$. EPA, eicosapentaenoic acid; AA, arachidonic acid.

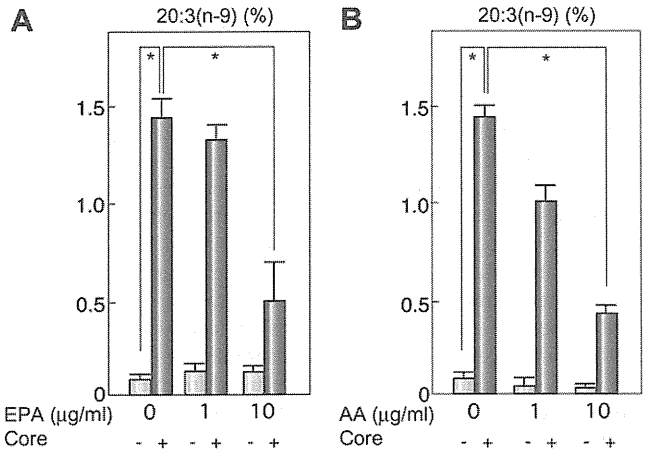

Fig. 4. Effect of EPA and AA on the concentration of 20:3(n-9). HepG2 cells with or without the core protein were incubated with EPA (A) or AA (B) for 48 h. The fatty acid compositions of the total cell lipids were analyzed and the percentages of the C20:3(n-9) fraction were measured. Light blue bars indicate control cells and dark blue bars indicate core-expressing cells. $N = 5$ in each group. $^{*}p < 0.05$.

suggested to be associated with HCV infection by the action of the HCV core protein [32–35]. Then, we explored the possibility that an increase in the NADH level, which is caused by the mitochondrial ETS dysfunction, induces the activation of fatty acid desaturases. Because fatty acid synthesis or fatty acid desaturation is accompanied by the oxidation of NAD(P)H, we measured the ketone body ratio (KBR) in the culture medium to estimate the redox state in the HepG2 cells expressing the core protein.

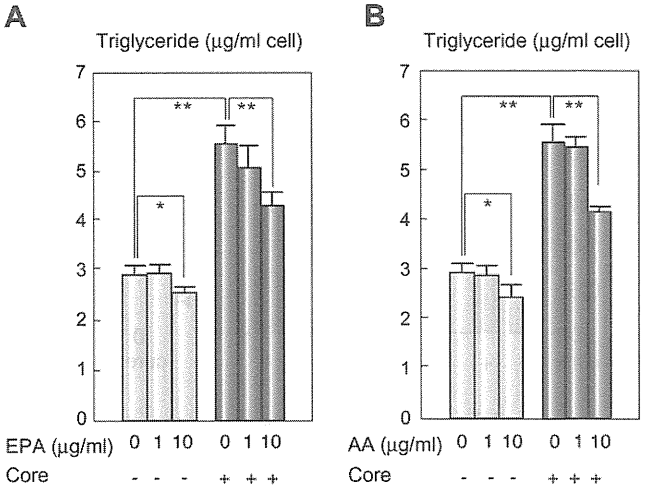

Fig. 5. Effect of EPA and AA on triglyceride content. HepG2 cells with or without the core protein were incubated with EPA (A) or AA (B) for 48 h. The triglyceride volume of the total cell lipids was measured and the triglyceride contents in the cells were calculated. Light blue bars indicate control cells and dark blue bars indicate core-expressing cells. $N = 5$ in each group. $^{*}p < 0.05$, $^{**}p < 0.01$.

The KBR, which is in equilibrium with the intramitochondrial NAD^+/NADH [26,36], in the culture medium of the core-expressing cells, was significantly lower than that of control cells (Fig. 6A, $p < 0.01$). The ratio of lactate to pyruvate (lactate/pyruvate), which is proportional to the cytosolic NADH/NAD^+ [26], in the culture medium of the core-expressing cells was significantly higher than that of control cells (Fig. 6B, $p < 0.05$). These results, the higher NADH/NAD^+ ratio in both determinations, indicate that NADH accumulates in the core-expressing HepG2 cells, resulting in the overreduced state, as a consequence of the core protein expression. The amounts of total ketone bodies were significantly higher in the core-expressing cells than that in the control cells (Fig. 6C).

Effects of pyruvate on lipid metabolism in core-expressing cells

The addition of pyruvate into this constitutive core protein expression system, in which the pyruvate metabolism is in equilibrium, is expected to cause a reduction in the NADH level along with increases in the levels of lactate and NAD^+, because pyruvate tends to be converted to lactate by the action of lactate dehydrogenase (LDH) under the condition of high NADH/NAD^+ ratio [26,36]. Actually, the addition of pyruvate into the culture medium at various concentrations increased the KBR and reduced the amount of 5,8,11-eicosatrienoic acid (20:3 (n-9)) (Fig. 6D, $p < 0.05$ at 10 mM pyruvate), while it had no effect on the control cells. It also caused a reduction in the amount of triglyceride in the core-expressing cells but not in the control cells (Fig. 6E). This finding strongly supports the notion that NADH accumulation is, at least, one of the causes of the activation of fatty acid desaturases in this HCV model. The mRNA levels of anti-oxidant genes significantly decreased after the incubation with pyruvate at 10 mM (catalase, 1.27 ± 0.06 vs. 0.91 ± 0.05; glutathione synthetase 1.39 ± 0.04 vs. 1.01 ± 0.06; glutathione peroxidase 1.48 ± 0.03 vs. 1.23 ± 0.07, pyruvate (−) vs. pyruvate (+), $p < 0.05$, respectively), suggesting that pyruvate reduced the levels of oxidative stress in the core-expressing HepG2 cells.

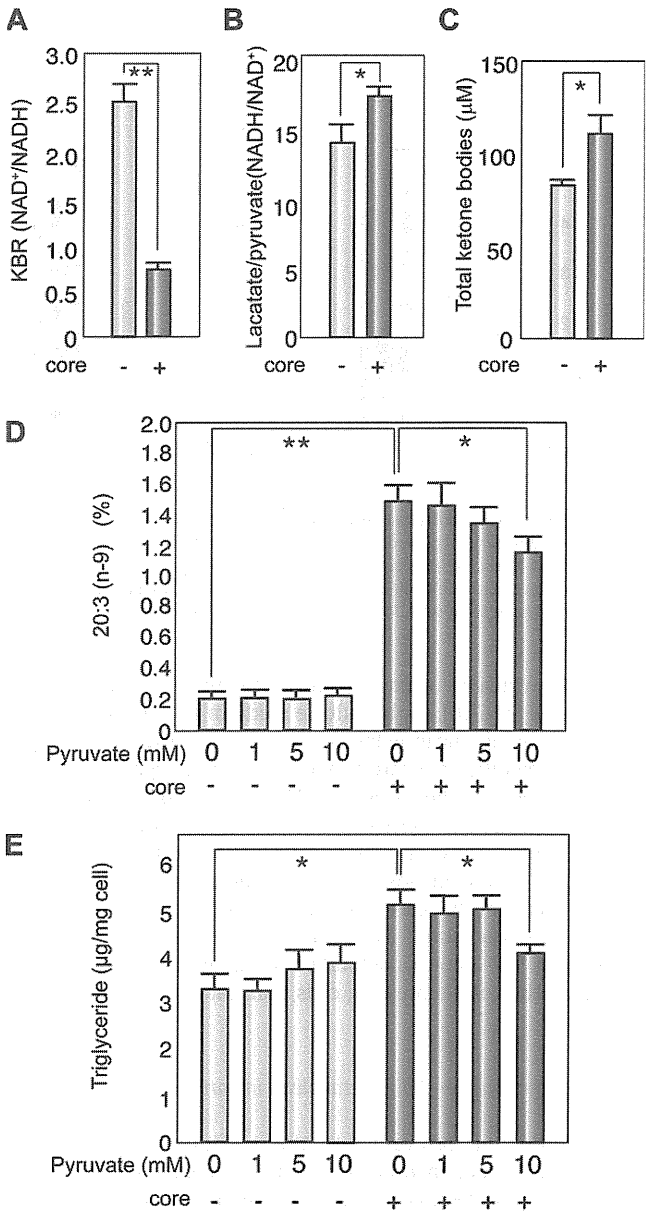

Fig. 6. NADH accumulation and effect of pyruvate in core-expressing cells. HepG2 cells with or without the core protein were subjected to the determination of ketone body ratio (A) and lactate/pyruvate ratio (B) for the precise estimation of NAD^+/NADH and NADH/NAD^+. (C) Total ketone bodies. (D) The percentages of the C20:3(n-9) fraction were measured after incubation with pyruvate at various concentrations. (E) The total amount of triglyceride was measured after incubation with pyruvate at various concentrations. Light blue bars indicate control cells and dark blue bars indicate core-expressing cells. $N = 5$ in each group. $^*p < 0.05$, $^{**}p < 0.01$.

Expression of SREBP-1 and desaturase genes in core-expressing cells

We previously showed that the core protein activates the expression of the SREBP-1c gene, which regulates the production of triglyceride [37] in the liver. We, therefore, examined the mRNA levels of genes associated with lipid metabolism in the current system. As shown in Fig. 7, the mRNA levels of SREBP-1c and delta-9 (stearoyl CoA) desaturase genes, but not that of the SREBP-1a gene, were significantly higher in the core-expressing cells than that in the control cells. Of note, the mRNA levels of the former two genes significantly decreased after the incubation with AA. The treatment with pyruvate also reduced the mRNA levels of the two genes, but the difference was not statistically significant compared with the control.

Discussion

The core protein of HCV modulated the activities of delta desaturases and changed the saturation states of fatty acids. The observed change in the HepG2 cells, namely, an increase in the amounts of unsaturated fatty acids, may support cell proliferation, by increasing the fluidity of the cell membrane as reported previously [20]. In the HepG2 cells expressing the core protein, the delta-6 desaturase activity was as high as that of the delta-9 desaturase, leading to the accumulation of a downstream product, 20:3(n-9) fatty acid. This was, unexpectedly, in contrast to our previous result on the liver tissues of HCV core gene transgenic mice, in which the 18:1/18:0 and 16:1/16:0 ratios were significantly higher than that in the liver tissues of normal littermate mice, indicating the activation of delta-9 desaturase [8]. The 16:1/16:0 and 18:1/18:0 ratios observed in the control HepG2 cells were consistent with the results of a previous study: the delta-6 desaturase activity is inherently higher in HepG2 cells than in normal mouse hepatocytes [28,29]. This may explain the difference in the effect of the core protein on lipid metabolism in these two systems, namely, HepG2 cells and mouse liver tissues. The significant increase in the delta-9 desaturase index and high concentration of 20:3(n-9) by the administration of ETYA, a delta-6 desaturase inhibitor, indicate the activation of delta-9 desaturase in the core-expressing cells. The results of real-time PCR analysis for determining the mRNA levels of these enzymes corroborated the current estimation of desaturase activities as determined by fatty acid analysis.

The mechanism underlying the activation of fatty acid desaturation by the HCV core protein is still unclear, but one possibility is the presence of an overreduced state in the core-expressing cells. The HCV core protein is closely associated with mitochondrial dysfunction, in particular, that of the respiratory chain complexes, resulting in an impairment of NADH oxidation [32–35]. NADH accumulation leads to an increase in desaturase activities through the augmentation of microsomal electron transfer [38]. In fact, the KBR in the core-expressing cells was significantly lower than that in the control cells, indicating the accumulation of NADH within the cells. The addition of pyruvate resulted in an increase in the KBR and a reduction in the amounts of triglyceride and 5,8,11-eicosatrienoic acid (20:3 (n-9)) while it had no effect on the control cells, strongly supporting the notion that NADH accumulation induced by the core protein is, at least, one of the causes of the activation of fatty acid desaturases in this HCV model.

Another possible mechanism underlying the accelerated desaturation is the activation of SREBP-1c, which controls the expression of delta-9 desaturase. In fact, the level of SREBP-1c mRNA was higher in the core-expressing cells than that in the control cells as reported previously [37]. The relief of NADH accumulation by pyruvate administration resulted in the reduced accumulation of triglyceride and unsaturated fatty acids, which was accompanied by the reduction in SREBP-1c and delta-9 desaturase gene expression levels. The intracellular accumulation of NADH might be involved in the activation of the SREBP-1c gene expression by the core protein. Thus, NADH accumulation, which

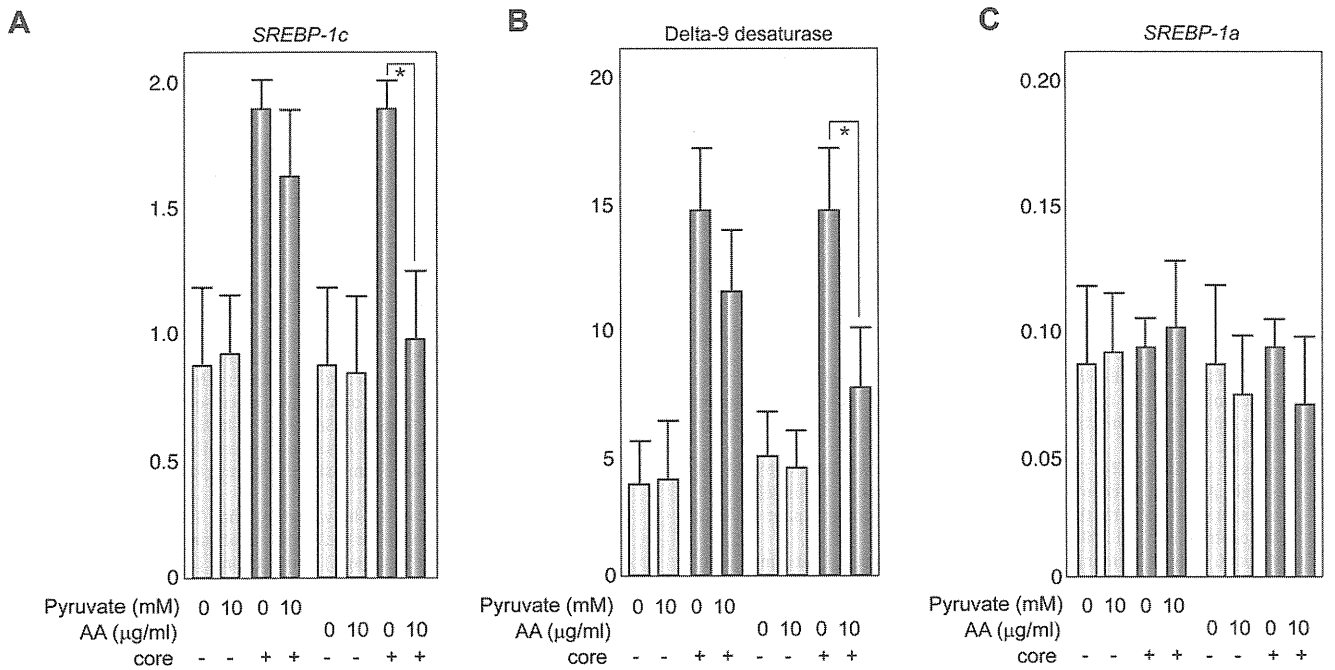

Fig. 7. Effect of pyruvate and AA on mRNA levels of lipid-associated genes. The mRNA levels of *SREBP-1c* (A), delta-9 desaturase (B) and *SREBP-1a* (C) genes were determined by real-time PCR analysis. The transcription of the genes was normalized with that of hypoxanthine phosphoribosyltransferase, and the values are expressed as relative activities. Light blue bars indicate control cells and dark blue bars indicate core-expressing cells. $N = 5$ in each group. $^{*}p < 0.05$. SREBP, sterol regulatory element binding protein.

is induced by the core protein through the impairment of the mitochondrial complex function [35], may be a key event that leads to the SREBP-1c activation, the desaturase activation, and the development of steatosis associated with HCV infection.

EPA and AA (PUFAs), which are known to suppress desaturase activities, lowered the 18:1/18:0 and 16:1/16:0 ratios and decreased the concentration of 20:3(n-9) concomitantly with that of triglyceride, regardless of the presence of the core protein, probably through SREBP-1c suppression (Fig. 7) [39]. On the other hand, the administration of EPA or AA did not affect the KBR in the core-expressing or control cells (data not shown), limiting the PUFAs ability to counteract the effect of the core protein. This is in contrast to the fact that the addition of pyruvate caused an increase in the KBR and a reduction in the amounts of triglyceride and 5,8,11-eicosatrienoic acid (20:3 (n-9)), while it had no effect on the control cells.

Fatty acid desaturation is closely associated with increased membrane fluidity [20], leading to augmented cell metabolism and higher cell division rates [21,22]. Although the relationship between carcinogenesis and lipid metabolism altered by the HCV core protein remains to be further clarified, alterations in lipid metabolism, in particular, in the desaturation of fatty acids, are closely associated with HCV infection, and PUFAs could prevent the pathogenesis of HCV-associated disorders involving lipid metabolism.

Conflict of interest

The authors who have taken part in this study declared that they do not have anything to disclose regarding funding or conflict of interest with respect to this manuscript.

Acknowledgments

This work was supported in part by Grant-in-Aid for Scientific Research on Priority Area from the Ministry of Education, Science, Sports, and Culture of Japan; Health Sciences Research Grants of The Ministry of Health, Labour, and Welfare (Research on Hepatitis); and a grant from The Sankyo Foundation of Life Science.

References

[1] Saito I, Miyamura T, Ohbayashi A, Harada H, Katayama T, Kikuchi S, et al. Hepatitis C virus infection is associated with the development of hepatocellular carcinoma. Proc Natl Acad Sci USA 1990;87:6547–6549.
[2] Schemer PJ, Ashrafzadeh P, Sherlock S, Brown D, Dusheiko GM. The pathology of chronic hepatitis C. Hepatology 1992;15:567–571.
[3] Bach N, Thung SN, Schaffner F. The histological features of chronic hepatitis C and autoimmune chronic hepatitis: a comparative analysis. Hepatology 1992;15:572–577.
[4] Fujie H, Yotsuyanagi H, Moriya K, Shintani Y, Tsutsumi T, Takayama T, et al. Steatosis and intrahepatic hepatitis C virus in chronic hepatitis. J Med Virol 1999;59:141–145.
[5] Moradpour D, Englert C, Wakita T, Wands JR. Characterization of cell lines allowing tightly regulated expression of hepatitis C virus core protein. Virology 1996;222:51–63.
[6] Barba G, Harper F, Harada T, Kohara M, Goulinet S, Matsuura Y, et al. Hepatitis C virus core protein shows a cytoplasmic localization and associates to cellular lipid storage droplets. Proc Natl Acad Sci USA 1997;94:1200–1205.
[7] Moriya K, Yotsuyanagi H, Shintani Y, Fujie H, Ishibashi K, Matsuura Y, et al. Hepatitis C virus core protein induces hepatic steatosis in transgenic mice. J Gen Virol 1997;78:1527–1531.
[8] Moriya K, Todoroki T, Tsutsumi T, Fujie H, Shintani Y, Miyoshi H, et al. Increase in the concentration of carbon 18 monosaturated fatty acids in the liver with hepatitis C: analysis in transgenic mice and humans. Biophys Biochem Res Commun 2001;281:1207–1212.
[9] Lerat H, Honda M, Beard MR, Loesch K, Sun J, Yang Y, et al. Steatosis and liver cancer in transgenic mice expressing the structural and nonstructural proteins of hepatitis C virus. Gastroenterology 2002;122:352–365.

[10] Naas T, Ghorbani M, Alvarez-Maya I, Lapner M, Kothary R, De Repentigny Y, et al. Characterization of liver histopathology in a transgenic mouse model expressing genotype 1a hepatitis C virus core and envelope proteins 1 and 2. J Gen Virol 2005;86:2185–2196.
[11] Adinolfi LE, Gambardella M, Andreana A, Tripodi MF, Utili R, Ruggiero G. Steatosis accelerates the progression of liver damage of chronic hepatitis C patients and correlates with specific HCV genotype and visceral obesity. Hepatology 2001;33:1358–1364.
[12] Massard J, Ratziu V, Thabut D, Moussalli J, Lebray P, Benhamou Y, et al. Natural history and predictors of disease severity in chronic hepatitis C. J Hepatol 2006;44:S19–S24.
[13] Leandro G, Mangia A, Hui J, Fabris P, Rubbia-Brandt L, Colloredo G, et al. HCV meta-analysis (on) individual patients' data study group. Relationship between steatosis, inflammation, and fibrosis in chronic hepatitis C: a meta-analysis of individual patient data. Gastroenterology 2006;130:1636–1642.
[14] Patton HM, Patel K, Behling C, Bylund D, Blatt LM, Vallee M, et al. The impact of steatosis on disease progression and early and sustained treatment response in chronic hepatitis C patients. J Hepatol 2004;40: 484–490.
[15] Harrison SA, Brunt EM, Qazi RA, Oliver DA, Neuschwander-Tetri BA, Di Bisceglie AM, et al. Effect of significant histologic steatosis or steatohepatitis on response to antiviral therapy in patients with chronic hepatitis C. Clin Gastroenterol Hepatol 2005;3:604–609.
[16] Moriya K, Fujie H, Shintani Y, Yotsuyanagi H, Tsutsumi T, Ishibashi K, et al. The core protein of hepatitis C virus induces hepatocellular carcinoma in transgenic mice. Nat Med 1998;4:1065–1067.
[17] Koike K. Molecular basis of hepatitis C virus-associated hepatocarcinogenesis: lessons from animal model studies. Clin Gastroenterol Hepatol 2005;3:S132–S135.
[18] Shi ST, Lee KJ, Aizaki H, Hwang SB, Lai MM. Hepatitis C virus RNA replication occurs on a detergent-resistant membrane that cofractionates with caveolin-2. J Virol 2003;77:4160–4168.
[19] Miyanari Y, Atsuzawa K, Usuda N, Watashi K, Hishiki T, Zayas M, et al. The lipid droplet is an important organelle for hepatitis C virus production. Nat Cell Biol 2007;9:1089–1097.
[20] Stubbs CD, Smith AD. The modification of mammalian membrane polyunsaturated fatty acid composition in relation to membrane fluidity and function. Biochim Biophys Acta 1984;779:89–137.
[21] Li J, Ding SF, Habib NA, Fermor BF, Wood CB, Gilmour RS. Partial characterization of a cDNA for human stearoyl-CoA desaturase and changes in its mRNA expression in some normal and malignant tissues. Int J Cancer 1994;57:348–352.
[22] Vinciguerra M, Carrozzino F, Peyrou M, Carlone S, Montesano R, Benelli R, et al. Unsaturated fatty acids promote hepatoma proliferation and progression through downregulation of the tumor suppressor PTEN. J Hepatol 2009;50:1132–1141.
[23] Ntambi JM. Regulation of stearoyl-CoA desaturase by polyunsaturated fatty acids and cholesterol. J Lipid Res 1999;40:1549–1558.
[24] Ruggieri A, Murdolo M, Harada T, Miyamura T, Rapicetta M. Cell cycle perturbation in a human hepatoblastoma cell line constitutively expressing hepatitis C virus core protein. Arch Virol 2004;149:61–74.
[25] Morrison WR, Smith LM. Preparation of fatty acid methyl esters and dimethylacetals from lipids with boron fluoride–methanol. J Lipid Res 1964;5:600–608.
[26] Williamson DH, Mellanby J, Krebs HA. Enzymic determination of D(-)-beta-hydroxybutyric acid and acetoacetic acid in blood. Biochem J 1962;82:90–96.
[27] Abid K, Pazienza V, Gottardi A, Rubbia-Brandt L, Conne B, Pugnale P, et al. An in vitro model of hepatitis C virus genotype 3a-associated triglycerides accumulation. J Hepatol 2005;42:744–751.
[28] Portolesi R, Powell BC, Gibson RA. Delta6 desaturase mRNA abundance in HepG2 cells is suppressed by unsaturated fatty acids. Lipids 2008;43:91–95.
[29] Choi Y, Park Y, Pariza MW, Ntambi JM. Regulation of stearoyl-CoA desaturase activity by the trans-10, cis-12 isomer of conjugated linoleic acid in HepG2 cells. Biochem Biophys Res Commun 2001;284:689–693.
[30] Strittmatter P, Spatz L, Corcoran D, Rogers MJ, Setlow B, Redline R. Purification and properties of rat liver microsomal stearyl coenzyme a desaturase. Proc Natl Acad Sci USA 1974;71:4565–4569.
[31] Joshi VC, Wilson AC, Wakil SJ. Assay for the terminal enzyme of the stearoyl coenzyme A desaturase system using chick embryo liver microsomes. J Lipid Res 1977;18:32–36.
[32] Korenaga M, Wang T, Li Y, Showalter LA, Chan T, Sun J, et al. Hepatitis C virus core protein inhibits mitochondrial electron transport and increases reactive oxygen species (ROS) production. J Biol Chem 2005;280: 37481–37488.
[33] Piccoli C, Scrima R, Quarato G, D'Aprile A, Ripoli M, Lecce L, et al. Hepatitis C virus protein expression causes calcium-mediated mitochondrial bioenergetic dysfunction and nitro-oxidative stress. Hepatology 2007;46:58–65.
[34] Tsutsumi T, Matsuda M, Aizaki H, Moriya K, Miyoshi H, Fujie H, et al. Proteomics analysis of mitochondrial proteins reveals overexpression of a mitochondrial protein chaperone, prohibitin, in cells expressing hepatitis C virus core protein. Hepatology 2009;50:378–386.
[35] Moriya K, Miyoshi H, Tsutsumi T, Shinzawa S, Fujie H, Shintani Y, et al. Tacrolimus ameliorates metabolic disturbance and oxidative stress caused by hepatitis C virus core protein: Analysis using mouse model and cultured cells. Am J Pathol 2009;175:1515–1524.
[36] Williamson DH, Lund P, Krebs HA. The redox state of free nicotinamide-adenine dinucleotide in the cytoplasm and mitochondria of rat liver. Biochem J 1967;103:514–527.
[37] Moriishi K, Mochizuki R, Moriya K, Miyamoto H, Mori Y, Abe T, et al. Critical role of PA28gamma in hepatitis C virus-associated steatogenesis and hepatocarcinogenesis. Proc Natl Acad Sci USA 2007;104:1661–1666.
[38] Jansson I, Schenkman JB. Studies on three microsomal electron transfer enzyme systems. Specificity of electron flow pathways. Arch Biochem Biophys 1977;178:89–107.
[39] Sekiya M, Yahagi N, Matsuzaka T, Najima Y, Nakakuki M, Nagai R, et al. Polyunsaturated fatty acids ameliorate hepatic steatosis in obese mice by SREBP-1 suppression. Hepatology 2003;38:1529–1539.

Liver INTERNATIONAL
OFFICIAL JOURNAL OF THE INTERNATIONAL ASSOCIATION FOR THE STUDY OF THE LIVER

Liver International ISSN 1478-3223

CLINICAL STUDIES

Intrahepatic bile duct dilatation after percutaneous radiofrequency ablation for hepatocellular carcinoma: impact on patient's prognosis

Yuji Kondo, Shuichiro Shiina, Ryosuke Tateishi, Toru Arano, Koji Uchino, Kennichiro Enooku, Eriko Goto, Hayato Nakagawa, Ryota Masuzaki, Yoshinari Asaoka, Hajime Fujie, Tadashi Goto, Masao Omata, Haruhiko Yoshida and Kazuhiko Koike

Department of Gastroenterology, Graduate School of Medicine, The University of Tokyo, Tokyo, Japan

Keywords
bile duct dilatation – hepatocellular carcinoma – radiofrequency ablation

Abbreviations
AFP, α-fetoprotein; CT, computed tomography; DCP, des-γ-carboxy prothrombin; HCC, hepatocellular carcinoma; MRI, magnetic resonance imaging; RFA, radiofrequency ablation.

Correspondence
Yuji Kondo, Department of Gastroenterology, Graduate School of Medicine, The University of Tokyo, Tokyo, Japan
Tel: +81 3 3815 5411
Fax: +81 3 3814 0021
e-mail: ykon-tky@umin.ac.jp

Received 9 October 2010
Accepted 7 November 2010

DOI:10.1111/j.1478-3231.2010.02415.x

Abstract

Background: Percutaneous radiofrequency ablation (RFA) has been widely accepted as an alternative to surgery for small hepatocellular carcinoma (HCC). In RFA, a portion of liver tissue surrounding tumour is also ablated to achieve a safety margin. The intrahepatic bile duct may be injured and result in chronic bile duct dilatation upstream of the injured site. However, the impact of such an injury on the overall prognosis has been unclear. *Methods:* Patients who showed bile duct dilatation following RFA were identified by a retrospective review of imaging studies. Each dilatation was classified as mild (limited to one hepatic subsegment) or severe (affecting two or more subsegments). The relation between the incidence of intrahepatic bile duct dilatation and HCC recurrence or survival was analysed using proportional hazard models. *Results:* Among 589 consecutive HCC patients treated with RFA, 70 (11.9%) and 21 (3.6%) patients showed mild and severe bile duct dilatation respectively. Patients with severe dilatation, but not those with mild dilatation, had lower survival and higher HCC recurrence than patients without dilatation. Severe dilatation, but not mild dilatation, was significantly associated with death [hazard ratio (HR) 2.17, $P = 0.035$] and recurrence (HR 2.89, $P < 0.001$). *Conclusion:* Whereas mild bile duct dilatation after RFA is clinically negligible, bile duct dilatation affecting two or more subsegments should be regarded as a complication that may affect the prognosis and should be observed carefully.

Hepatocellular carcinoma (HCC) is one of the most common cancers worldwide (1, 2). Apart from liver transplantation, surgical resection is the optimal treatment of choice for HCC. However, the majority of HCC patients have background chronic liver diseases, especially cirrhosis, and a substantial proportion of patients are not eligible for surgical resection because of impaired liver function and/or multinodularity of the tumour. In such patients, less invasive percutaneous tumour ablation procedures have been applied, such as ethanol injection, microwave coagulation and radiofrequency ablation (RFA) (3, 4). Among them, RFA is currently the most widely accepted alternative to surgery because of its safety and high efficacy (5, 6).

The RFA applies thermal energy converted from radiofrequency current to the coagulation of tumour tissues. However, the thermal energy may also affect intra- and extrahepatic tissues, resulting in complications specific to RFA (7). We have characterized haemorrhagic complications following RFA (8), such as haemoperitoneum and haemothorax, and reported techniques such as intraperitoneal fluid infusion to prevent extrahepatic thermal injuries (9). Intrahepatic bile duct dilatation may appear several months after RFA. The dilatation is thought to represent downstream bile duct stricture caused by RFA-related thermal injuries. Thus, intrahepatic bile duct dilatation, or thermal injury to intrahepatic bile ducts, is another complication specific to RFA, which has not been well characterized.

In RFA, thermal energy is generated concentrical to the electrode and inevitably affects the surrounding liver parenchyma. In fact, we usually ablate a portion of surrounding liver intentionally to achieve sufficient safety margin. Blood vessels are thought to be relatively immune to the thermal injury because of the cooling effect of circulating fluid. On the other hand, the velocity of bile juice in the bile duct is much slower, and intrahepatic bile ducts near the tumour are prone to thermal injury during RFA. However, the injury to bile ducts cannot be recognized until some macroscopic changes, such as bile duct dilatation upstream of stenosis because of thermal injury, become visible on imaging

© 2010 John Wiley & Sons A/S

studies. Minimal injuries without visible ductal dilatation cannot be recognized, and such injuries seem to have little clinical significance. Recognizable bile duct dilatation that appears after RFA is not rare, reported to be found in 17% of patients (10). However, its impact on patient's prognosis remains unknown. In the current study, we sought to evaluate the effects of thermal injuries to intrahepatic bile ducts by comparing the survival rate and the HCC recurrence rate between patients with and without visible bile duct dilatation after RFA.

Patients and methods

Patients

Between January 2003 and December 2007, a total of 589 patients with HCC received RFA as the initial treatment at the Department of Gastroenterology, University of Tokyo Hospital. All patients were prospectively registered on an electronic database, and the current study was based on data observed until the end of December 2008. The flowchart of the current study is presented in Figure 1. Each patient underwent contrast-enhanced computed tomography (CT) or magnetic resonance imaging (MRI) about every 4 months after RFA for the screening of HCC recurrence. In the current study, those imaging studies were reviewed retrospectively to identify intrahepatic bile duct dilatation after RFA. We placed no restriction on RFA solely by the location of tumours (11). Thus, tumours adjacent to an intrahepatic bile duct, possibly at a high risk for bile duct injury, were also treated with RFA, if other conditions met the indication criteria for RFA, as described below.

Hepatocellular carcinoma was diagnosed mainly based on the typical findings on diagnostic imaging, i.e., hyperattenuation in the arterial phase and hypo-attenuation in the portal-venous phase on contrast-enhanced dynamic CT or MRI (12). Percutaneous needle biopsy was reserved for tumours not typical on imaging studies.

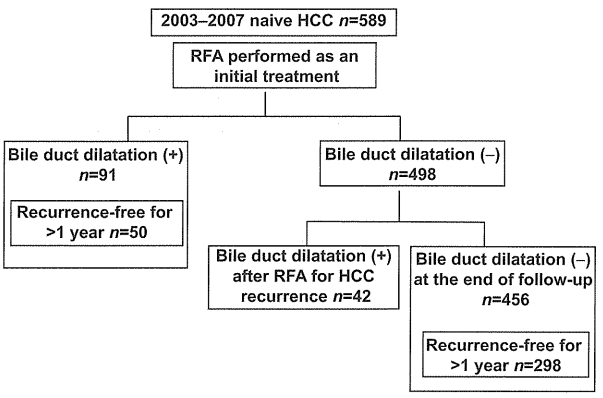

Fig. 1. Schematic flowchart of the study. HCC, hepatocellular carcinoma; RFA, radiofrequency ablation.

Radiofrequency ablation

The inclusion criteria for RFA in the author's institution were as follows: tumour size not larger than 3 cm in diameter, tumour number not more than three, absence of vascular invasion or extrahepatic metastasis, serum total bilirubin concentration not higher than 3 mg/dl, platelet count no less than $50 \times 10^3/mm^3$, prothrombin activity no less than 50% (approximately 1.5 INR) and absence of uncontrollable ascites. Patients with a prior history of bilioenteric anastomosis or sphincterotomy were excluded because these conditions were risk factors for hepatic abscess formation after RFA. RFA was sometimes performed on patients with a tumour size larger than 3 cm or tumour number more than three, when RFA could be expected to improve survival after careful consideration. A written informed consent was obtained from each patient, and family members when appropriate, before RFA.

The RFA was performed on an in-patient basis. The details of the RFA procedure have been described elsewhere (13). In summary, RFA was performed with a 17 G internally cooled electrode system (Valleylab, Boulder, CO, USA) (14, 15) with a 2 or 3 cm exposed tip, which was inserted under real-time ultrasound guidance. Intrapleural or intraperitoneal fluid infusion was performed before electrode needle insertion, if appropriate, according to the previous reports (9, 16). RFA was started at 60 and 40 W for the 3 and 2 cm exposed tips, respectively, and the power was increased in a stepwise fashion by 20 W/min. The duration of a single ablation was 12 min for the 3 cm electrode and 6 min for the 2 cm electrode.

Dynamic CT was performed within 3 days after treatment. Complete tumour necrosis was defined as hypo-attenuation of the entire lesion with a sufficient surrounding margin. Patients received additional RFA until complete necrosis was confirmed. After complete tumour ablation, patients were followed up at the outpatient clinic every 4 months with enhanced three-phase dynamic CT or MRI. In the current study, all these CT images performed in the follow-up period were reviewed for the presence of any intrahepatic bile duct dilatation. Patients who had HCC recurrence were treated with RFA again or transcatheter arterial chemoembolization appropriately according to the tumour size and number, liver function reserve and general medical conditions.

Definition of bile duct dilatation

Bile duct injury can be recognized only as an upstream distal bile duct dilatation on imaging studies. In the current study, any disproportional dilatation of intrahepatic bile ducts, including biloma, in the upstream of the ablated area that was newly detected on dynamic enhanced CT or MRI after RFA was defined as a bile duct injury because of RFA. This definition was in accordance with the previous study by Kim *et al.* (10). Dilatation of a bile duct that had existed before the initial RFA, or that

© 2010 John Wiley & Sons A/S

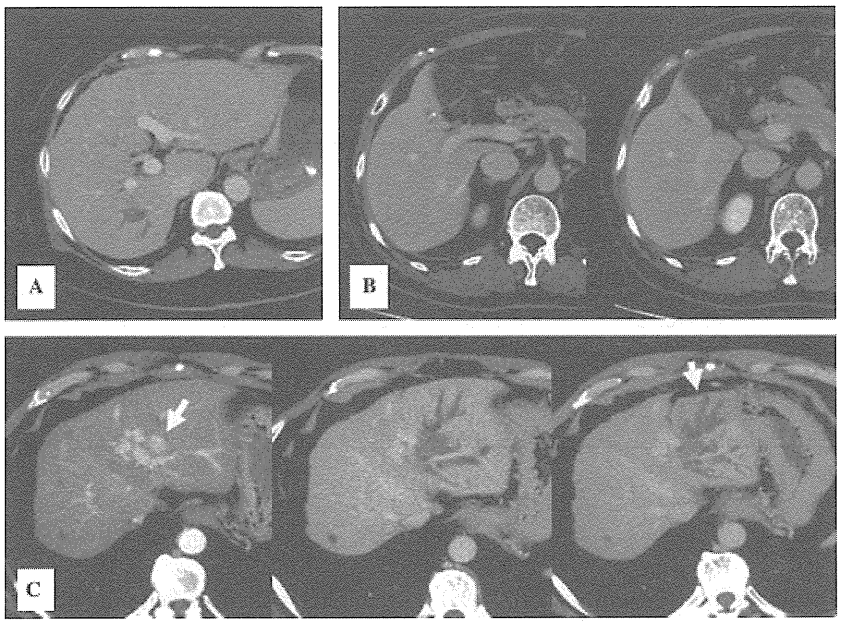

Fig. 2. Typical cases with bile duct dilatation after radiofrequency ablation (RFA); (A) 63-year-old male with peripheral bile duct dilatation after RFA for hepatocellular carcinoma (HCC) in Segment 7; (B) 67-year-old male with subsegmental bile duct dilatation after RFA for hepatocellular carcinoma in Segment 5. (C) 49-year-old male with segmental bile duct dilatation. Left: HCC located adjacent to the Glisson's capsule, 2.2 cm in diameter, was detected (arrow) in a patient with cirrhosis because of hepatitis C infection. Middle: intrahepatic bile ducts (B2 and B3) were markedly dilated 4 months after RFA. Right: atrophy of hepatic parenchyma in the lateral segment was noted 1 year after RFA (arrow), without any recurrence of HCC.

was because of other mechanical process, such as biliary invasion of HCC, was not considered as an event of bile duct dilatation in the current study.

The bile duct dilatations found in the current study were divided into two categories, mild or severe, according to the distribution of dilated bile ducts. Mild dilatation was defined as dilatation limited to one hepatic subsegment, whereas severe dilatation was defined as dilatation in two or more subsegments. Some typical cases are presented in Figure 2. The extent of bile duct dilatation was judged on the last CT/MRI performed in the follow-up period.

Statistical analyses

Comparisons of the two groups were performed with Student's *t*-test for continuous variables and Fisher's exact test for frequency distributions. The survival curves were created with the Kaplan–Meier method. Two survival curves were compared with log-rank test. A *P*-value < 0.05 on a two-tailed test was considered statistically significant. To predict death and recurrence after RFA, a proportional hazard model was used, which included the severity of bile duct dilatation, age, gender, hepatitis C virus, Child–Pugh classification of liver function, maximum tumour size, tumour number, α-fetoprotein (AFP) and des-γ-carboxy prothrombin (DCP) as independent variables in univariate analyses. Severity of bile duct dilatation was treated as a trichotomous variable (none, mild or severe) and analysed using two dummy variables. In multivariate analyses, the two dummy variables were included together with variables with *P*-value < 0.05 in univariate analyses. All statistical analyses were performed using JMP 8 (SAS institute Japan, Tokyo, Japan) software.

Results

Patient characteristics

Of 589 patients, bile duct dilatation because of the initial RFA developed in 91 (15%) patients during the observation period. There were 70 patients with mild dilatation (limited to one subsegment; incidence among all patients, 11.9%) and 21 patients with severe dilatation (affecting two or more subsegments; 3.6%). There were 42 (7.1%) additional patients with bile duct dilatation that was detected after RFA for recurrent HCC, which we assumed to be because of the latter RFA. These 42 patients were excluded from the survival analyses because the impacts on the prognosis of the bile duct injury and HCC recurrence were indistinctive in these patients, whereas in analyses of recurrence after initial RFA, they were included in the control (without bile duct injury) group because bile duct dilatation was not related to the first recurrence in these patients. The remaining 456 patients had not developed any bile duct dilatation until the end of follow-up. The interval between the initial RFA and the detection of bile duct dilatation was shorter than 6 months in 70 (77%), 6–12 months in 13 (14%),

© 2010 John Wiley & Sons A/S

Table 1. Baseline characteristics of patients with or without bile duct injury

		After initial RFA ($n=91$)					
Bile duct dilatation	Absent ($n=456$)	Mild ($n=70$)	P	Severe ($n=21$)	P	After RFA for recurrence ($n=42$)	P
Mean age (year)	68.4 (8.43)	69.2 (8.08)	0.44	68.7 (10.24)	0.90	69.0 (7.61)	0.64
Age (< 70/≥70)	252/204	38/32	0.90	11/10	0.83	23/19	1.00
Gender (male/female)	295/161	42/28	0.50	16/5	0.35	24/18	0.40
HCV (positive/negative)	346/110	48/22	0.24	16/5	1.00	35/7	0.34
Child–Pugh grade (A/BC)	334/122	46/24	0.20	16/5	0.81	28/14	0.37
Tumour size (< 2cm/≥2cm)	189/267	23/47	0.19	6/15	0.27	13/29	0.19
Tumour diameter (cm)	2.45 (10.15)	2.42 (7.58)	0.78	2.79 (11.34)	0.14	2.31 (6.03)	0.43
Tumour number (= < 2/≥3)	362/94	55/15	1.00	15/6	0.41	32/10	0.69
Mean tumour number	1.78 (1.16)	1.87 (1.26)	0.53	2.33 (1.96)	0.04	1.69 (1.02)	0.57
AFP (< /≥100 (ng/ml)	370/86	51/19	0.11	16/5	0.78	33/9	0.84
DCP (< /≥100 (mAU/ml)	385/71	53/17	0.08	16/5	0.36	38/5	0.52

Continuous variables are presented as mean (SD).

AFP, α-fetoprotein; DCP, des-γ-carboxy prothrombin; HCV, hepatitis C virus; RFA, radiofrequency ablation.

1–2 years in 6 (7%) and beyond 2 years in two (2%) patients. Bile duct dilatation was found in the left lobe in 43, the right lobe in 45 and was bilobular in three patients.

The characteristics of the included patients immediately before the initial RFA are presented in Table 1. Most characteristics did not differ significantly between patients who subsequently presented bile duct dilatation and those who did not. However, the mean number of tumours was significantly greater in patients with severe bile duct dilatation than in those without dilatation (2.33 vs. 1.78, $P=0.04$).

The details of the 21 patients with severe bile duct dilatation are presented in Table 2. In 19 of them, the tumour was adjacent to a major portal venous branch, namely, the umbilical portion of the left portal branch, the right anterior branch or the right posterior branch. Because portal veins and intrahepatic bile ducts run parallel in the liver, we can assume that these tumours were also adjacent to the corresponding bile ducts. The remaining two patients had a tumour adjacent to two subsegmental branches. HCC recurrence after curative ablation was identified in 18 patients, two with local tumour progression, 15 with intrahepatic recurrence distant from the primary tumour and the remaining one with extrahepatic metastasis.

To assess the relationship between tumour location and the incidence of severe bile duct dilatation, 302 patients with uninodular HCC were analysed. The incidence of severe bile duct dilatation was 0% (0/5), 6.5% (3/46), 0% (0/35), 0.7% (1/143) and 4.1% (3/73) in patients with a tumour located in the caudate lobe (Segment 1), the left lateral segment, the left medial segment, the right anterior segment and the right posterior segment respectively. Although statistical analysis was not applicable because of the small number of patients with severe bile duct dilatation, tumours located in the left lateral or the right posterior segment seemed to be at a higher risk of developing severe bile duct dilatation after RFA.

Impact of bile duct dilatation on liver function

To assess the impact of bile duct dilatation after RFA on liver function reserve, changes in serum albumin and the total bilirubin concentrations 6 months and 1 year after RFA were calculated. Those patients who had HCC recurrence within 1 year after the ablation were excluded from this analysis of liver function changes because HCC recurrence and its treatment may have affected liver function and obscured the impact of bile duct dilatation induced by the initial RFA. HCC recurrence occurred within 1 year after the initial RFA in 158 of 456 patients without bile duct dilatation, 30 of 70 patients with mild dilatation and 11 of 21 patients with severe dilatation. Thus, 50 patients with bile duct dilatation (40 with mild dilatation and 10 with severe dilatation) and 298 patients without were analysed. No patients died without HCC recurrence within 1 year after the initial RFA. The baseline characteristics did not differ between the patients with mild or severe bile duct dilatation and those without (data not shown), except that DCP > 100 was more frequent in patients with mild dilatation than in patients without bile duct dilatation ($P=0.03$).

The changes in the serum albumin concentration in the three groups (patients without dilatation, patients with mild dilatation and patients with severe dilatation) are presented in Table 3. The baseline value and the decrease in 6 months were not different among the three groups. However, the decrease in 1 year was significantly greater in patients with mild or severe dilatation. The changes in the serum total bilirubin concentration are presented in Table 3. The baseline value was greater in patients with mild dilatation than that in patients without dilatation. The increase in the total bilirubin concentration in 6 months was significantly greater in the

© 2010 John Wiley & Sons A/S

Table 2. The 21 patients with severe bile duct dilatation

Patients	Age	Gender	Maximum tumour diameter (mm)	Tumour number	Tumour location*	Adjacent portal venous branches†	Affected subsegments	Recurrence‡	Time to recurrence (year)	Type of first recurrence§	Observation period (year)	outcome	Cause of death‖
1	65	M	40	2	8	A	5, 6, 7, 8	+	0.9	Distant	5.4	Dead	HF
2	69	M	22	1	3	U	2, 3	+	1.3	Local	5.5	Censored	
3	66	F	24	2	3	U	2, 3	+	0.7	Distant	4.9	Dead	HCC
4	66	M	22	3	7	P	5, 7, 8	+	0.8	Distant	4.1	Censored	
5	77	M	51	10	2	U	2, 3	NA	–	–	2.5	Dead	HCC
6	64	M	18	2	2	U	2, 3	+	0.6	Extrahepatic	4.6	Dead	HCC
7	64	M	16	2	5	A, P	5, 6, 7, 8	+	1.4	Distant	3.9	Dead	HCC
8	79	M	29	3	4, 8	4, A, 6	4, 5, 6, 8	+	0.4	Distant	3.4	Dead	HCC
9	57	F	26	2	4	U	2, 3, 4	+	2.4	Distant	3.7	Censored	
10	78	M	21	6	2	U	2, 3	NA	–	–	1.2	Dead	HF
11	79	F	40	2	4	U	2, 3	+	0.3	Distant	1.1	Dead	HF
12	76	M	18	2	8	A, P	5, 8	+	0.5	Distant	2.9	Censored	
13	84	M	50	1	6	P	6, 7	+	0.4	Local	1.2	Dead	HCC
14	72	F	19	2	5	5	5, 8	+	1.2	Distant	2.9	Censored	
15	73	M	16	1	2	U	2, 4	+	1.2	Distant	2.5	Censored	
16	79	F	24	3	8	5, 8	5, 8	+	0.8	Distant	2.5	Censored	
17	57	M	18	3	2, 5	U, A	2, 5	+	0.9	Distant	1.4	Dead	HF
18	76	M	41	1	7	P	6, 7	+	0.9	Distant	1.8	Censored	
19	46	M	27	1	7	P	6, 7	+	1.0	Distant	1.1	Censored	
20	49	M	21	1	3	U	2, 3	+	1.6	Distant	1.7	Censored	
21	65	M	43	1	8	A	5, 8	–	–	–	1.3	Censored	

*The subsegment in which the tumour responsible for severe bile duct dilatation was mainly located.

†Portal venous branches to which the tumour was adjacent on CT or MRI were presented. U, umbilical portion of the left portal vein; A, right anterior branch; P, right posterior branch.

‡Patients 5 and 10 were treated without a curative intent because of tumour multiplicity. +, present; –, absent; NA, not applicable.

§Distant, intrahepatic recurrence distant from the primary tumour(s); local, local tumour progression; extrahepatic, extrahepatic tumour metastasis.

‖CT, computed tomography; HCC; hepatocellular carcinoma progression; HF, hepatic failure; MRI, magnetic resonance imaging.

Liver International (2010)
© 2010 John Wiley & Sons A/S

Table 3. Change of serum albumin and the total bilirubin concentration in 6 months and 1 year after the initial radiofrequency ablation in patients without any recurrence for at least 1 year

Bile duct dilatation	Absent ($n=298$)	Mild ($n=40$)	P	Severe ($n=10$)	P
Albumin (g/dl)					
Value before RFA	3.71 (0.44)	3.72 (0.46)	0.88	3.70 (0.45)	0.90
Change in 6 months	−0.03 (0.28)	−0.04 (0.23)	0.86	−0.02 (0.23)	0.95
Change in 1 year	−0.06 (0.31)	−0.35 (0.96)	< 0.01	−0.25 (0.31)	0.01
Total bilirubin (mg/dl)					
Value before RFA	0.88 (0.44)	1.14 (0.72)	< 0.01	1.00 (0.82)	0.41
Change in 6 months	+0.13 (0.31)	+0.31 (0.71)	< 0.01	+0.13 (0.16)	0.67
Change in 1 year	+0.18 (0.58)	+0.15 (0.35)	0.80	+0.28 (0.26)	0.27

Data are presented as mean (SD).

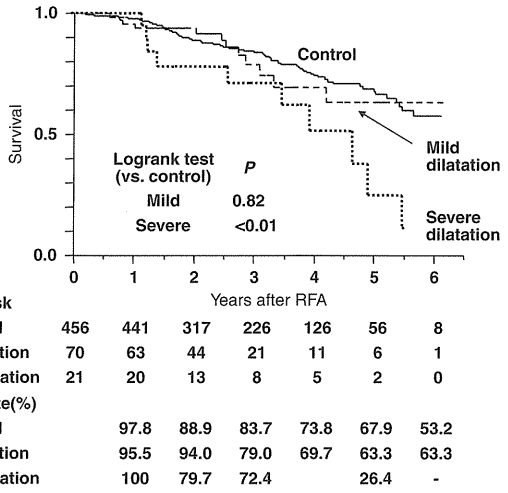

Fig. 3. Cumulative survival of patients with mild and severe bile duct dilatation compared with those without bile duct dilatation. RFA, radiofrequency ablation.

patients with mild dilatation than in those without dilatation. However, the increase was not different between patients with severe dilatation and patients without dilatation, and the increase in 1 year was not different among the three groups.

Survival after radiofrequency ablation in patients with and without bile duct dilatation

The overall survival was compared between patients with and without bile duct dilatation, excluding those who showed dilatation only after RFA for HCC recurrence ($n=42$). The survival curves created with Kaplan–Meier method are presented in Figure 3. The survival of patients with mild bile duct dilatation was not significantly different from that of patients without bile duct dilatation (control group). However, the survival of patients with severe bile duct dilatation was significantly lower ($P < 0.001$ by the log-rank test) than that of the control group. Ten out of 21 patients with severe bile duct dilatation died during the study period. The cause of death was hepatic failure in spite of controlled HCC in four and HCC progression in six patients.

The results of univariate and multivariate analyses to predict death based on proportional hazard model are presented in Table 4. In the univariate analysis, severe bile duct dilatation, age (older than 70), Child–Pugh classification (B or C), tumour number (more than three), AFP (> 100ng/ml) and DCP (> 100 mAu/ml) before RFA were selected as potential predictors of death. In the multivariate analysis, mild bile duct dilatation vs. no dilation, severe dilatation vs. no dilatation, together with other clinical factors, were used as independent variables. Although mild bile duct dilatation was not significant [hazard ratio (HR) 1.01, $P=0.973$], severe bile duct dilatation was one of the significant predictors of death (HR 2.17, $P=0.035$). In addition to severe bile duct dilatation, hepatitis C virus positivity, Child–Pugh classification (B/C vs. A) and tumour number (≥ 3) were significant predictors of death.

Hepatocellular carcinoma recurrence after radiofrequency ablation in patients with and without bile duct dilatation

In the analysis of HCC recurrence, patients with bile duct dilatation after RFA for recurrence, who were excluded from the survival above analyses, were combined with patients without bile duct dilatation (control). Patients treated by RFA without a curative intent were excluded (one from the mild dilatation group, two from the severe dilatation group and 13 from the control group), and thus 69 patients with mild bile duct dilatation, 19 with severe dilatation and 485 without dilatation (control) were analysed. Patients who died without HCC recurrence (two in the mild dilatation group, two in the severe dilatation group and 31 in the control group) were treated as censored.

The curves of cumulative HCC recurrence created with the Kaplan–Meier method are presented in Figure 4. The cumulative recurrence did not differ significantly between patients with mild bile duct dilatation and the controls, whereas patients with severe dilatation showed significantly higher cumulative recurrence than the controls ($P < 0.001$). During the study period, all 19 patients

© 2010 John Wiley & Sons A/S

Table 4. Univariate and multivariate analyses to predict death using the Cox proportional hazard model

	Univariate analysis			Multivariate analysis		
Variables at the initial RFA	HR	95% CI	*P*	HR	95% CI	*P*
Bile duct dilatation						
None	1			1		
Mild	1.04	0.54–1.82	0.889	1.01	0.52–1.77	0.973
Severe	2.45	1.20–4.46	0.017	2.17	1.06–3.96	0.035
Age (year) > 70	1.43	1.00–2.04	0.050			
Gender, male	1.24	0.85–1.85	0.261			
Hepatitis C virus (+)	1.56	1.01–2.51	0.045	1.60	1.62–3.34	0.040
Child–Pugh classification, B or C	2.63	1.83–3.74	< 0.001	2.33	1.62–3.34	< 0.001
Maximum tumour size > 2.0cm	1.33	0.93–1.95	0.122			
Tumour number ≥3	2.27	1.55–3.28	< 0.001	1.95	1.32–2.84	< 0.001
AFP (ng/ml) ≥100	1.62	1.06–2.38	0.024	1.44	0.94–2.15	0.090
DCP (mAu/ml) ≥100	1.77	1.13–2.67	0.013	1.63	1.03–2.50	0.037

AFP, α-fetoprotein; CI, confidence interval; DCP, des-γ-carboxy prothrombin; HR, hazard ratio; RFA, radiofrequency ablation.

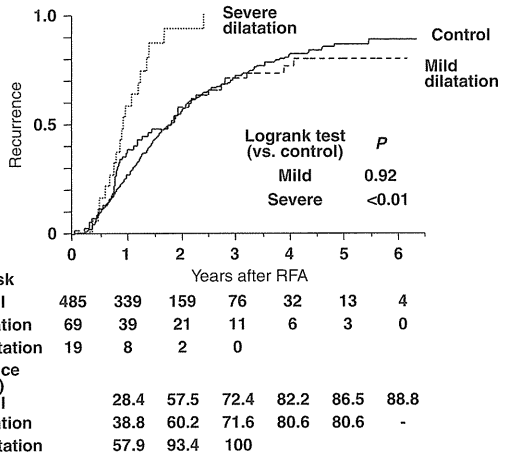

Fig. 4. HCC recurrence rates in patients with mild and severe bile duct dilatation compared with those without bile duct dilatation. HCC, hepatocellular carcinoma; RFA, radiofrequency ablation.

with severe bile duct dilatation developed HCC recurrence, local tumour progression in one, recurrence in the same subsegment as the bile duct dilatation in four, the same segment in two, other segments in 10, portal vein invasion in one and extrahepatic metastasis in one patient.

The results of univariate and multivariate analyses using the proportional hazard model are presented in Table 5. In the univariate analysis, severe bile duct dilatation, hepatitis C virus positivity, Child–Pugh classification (B or C), maximum tumour size (> 2.0 cm), tumour number (more than three), AFP (> 100 ng/ml) and DCP (> 100 mAu/ml) before RFA were selected as potential predictors of recurrence. Multivariate analysis was performed as in the analysis of overall survival shown above. Mild bile duct dilatation was not a significant predictor of recurrence (HR 1.01, $P = 0.959$), whereas severe bile duct dilatation was significant (HR 2.89, $P < 0.001$). Other significant predictors of recurrence were hepatitis C virus positivity, Child–Pugh classification (B or C), maximum tumour size (> 2.0 cm), tumour number (more than three), AFP (> 100 ng/ml) and DCP (> 100 mAu/ml).

Discussion

In the current study with a long-term follow-up, bile duct dilatation was found in 15% of patients who underwent RFA for HCC. However, most cases of bile duct dilatation were limited to a single subsegment of the liver, and we did not find a significant influence of such dilatation on the overall survival or HCC recurrence. However, severe bile duct dilatation, defined as dilatation in two or more subsegments, developed in 21/589 (3.6%) patients and this was shown to be associated with poorer survival and a higher incidence of HCC recurrence. Thus, severe bile duct dilatation should be regarded as a long-term complication of RFA, and patients who developed severe bile duct dilatation should be followed carefully. However, because the incidence of severe bile duct dilatation was acceptably low, the indication of RFA should not be restricted solely for fear of bile duct injury, at least in highly experienced institutions.

The liver function was slightly but significantly deteriorated in HCC recurrence-free patients with bile duct dilatation after RFA, although this patient selection may lead to underestimation of the deterioration of liver function. The decrease in the serum albumin concentration in 1 year, but not in the first 6 months, following RFA was significantly greater in patients with than in patients without bile duct dilatation. Patients with bile duct dilatation seem to show slow progressive impairment in hepatic function and the deterioration of liver function in the longer term may be more severe. In the current study, four of 10 patients with severe bile duct dilatation died of hepatic failure while HCC was well controlled. Admittedly, in order to elucidate the

© 2010 John Wiley & Sons A/S

Table 5. Univariate and multivariate analyses to predict recurrence using the Cox proportional hazard model

	Univariate analysis			Multivariate analysis		
Variables at initial RFA	HR	95% CI	*P*	HR	95% CI	*P*
Bile duct dilatation						
None	1			1		
Mild	1.09	0.78–1.47	0.603	1.01	0.72–1.37	0.959
Severe	2.94	1.75–4.63	< 0.001	2.89	1.72–4.55	< 0.001
Age (year) > 70	0.98	0.80–1.19	0.814			
Gender, male	0.97	0.80–1.20	0.800			
Hepatitis C virus (+)	1.31	1.04–1.67	0.023	1.41	1.10–1.82	0.007
Child–Pugh classification, B or C	1.38	1.10–1.71	0.005	1.36	1.07–1.72	0.013
Maximum tumour size > 2.0cm	1.29	1.06–1.58	0.012	1.23	0.98–1.54	0.07
Tumour number ≥3	1.73	1.37–2.17	< 0.001	1.63	1.26–2.08	< 0.001
AFP (ng/ml) ≥100	1.42	1.11–1.79	0.005	1.43	1.10–1.84	0.009
DCP (mAu/ml) ≥100	1.65	1.27–2.12	< 0.001	1.60	1.20–2.10	0.002

AFP, α-fetoprotein; CI, confidence interval; DCP, des-γ-carboxy prothrombin; HR, hazard ratio; RFA, radiofrequency ablation.

mechanism by which liver function deteriorates in patients with severe bile duct dilatation, the current study was limited by the small number of such patients. However, exacerbated liver dysfunction in the liver parenchyma upstream of bile duct stricture because of cholestasis may be a likely possibility.

In this series, four patients (Patient 1, 10, 11 and 17 in Table 2) died of hepatic failure although HCC was well controlled. Not surprisingly, patients with impaired liver function before RFA seem to be prone to hepatic failure because of severe bile duct dilatation. In fact, patients 10 and 17 had moderate cirrhosis, and the bile duct injury seemed to accelerate liver dysfunction. Patient 11 had aggressive HCC in severe cirrhotic liver, which required repeated RFA and transcatheter arterial chemoembolization. She died of hepatic failure probably because of treatment-related liver damage. On the other hand, Patient 1 had good liver function reserve before the initial RFA. He developed frequent HCC recurrence and RFA was repeated. Continuous percutaneous bile duct drainage was required for jaundice 3 years after the initial RFA, and he died of hepatic failure at 5.4 years. In patients who already have had severe bile duct dilatation, impairment of hepatic function by the treatment procedure for HCC recurrence was more severe, especially when the procedure was repeated. Therefore, treatment for recurrence should be planned carefully in such patients.

In the current study, severe bile duct dilatation was also found to be associated with a higher incidence rate of HCC recurrence, which may have worsened the prognosis of such patients. Six of 10 patients with severe bile duct dilatation died of HCC progression. The reason for this association between severe dilatation and a higher recurrence rate is unclear. It may be postulated that tumours adjacent to major intrahepatic bile ducts may be prone to receive insufficient ablation and consequently the recurrence rate is high. However, in the current study, only two patients developed local tumour progression among the 19 radically treated patients complicated with severe bile duct injury. Another possible explanation is that tumours associated with bile duct injury on RFA are more likely to have an invasive nature, namely, microscopic invasion into Glisson's capsule, portal vein or bile duct, which may have been accompanied by undetectable intrahepatic or extrahepatic metastases at the time of RFA.

Therefore, the worse prognosis of the patients with severe dilatation may be attributed not only to deterioration of liver function because of bile duct injury itself but also a higher rate of HCC recurrence. Considering that HCC progression and hepatic failure (in spite of controlled HCC) were found approximately equally to be patients' cause of death, these two factors had a similar impact on the prognosis of these patients.

Two distinct procedures have been reported for the prevention of bile duct injury by RFA, namely, prophylactic biliary stent placement and intraductal cooling of biliary duct with chilled saline during RFA (17–20), neither of which were used in the current study. These techniques require an endoscopic transpapillary insertion of a biliary drainage tube or laparotomy, which can be complicated by bleeding, pancreatitis or cholangitis. Such an invasive and complex nature may preclude further acceptance of these procedures as a routine for the prevention of bile duct injury, considering particularly the low incidence of severe bile duct dilatation. At present, the indication of such procedures should be carefully considered in each individual case. For tumours with an extremely high risk of developing severe bile duct dilatation after RFA, a percutaneous ethanol injection may be a safer alternative, although it may require more treatment sessions and higher technical expertise to ensure complete necrosis of the tumour (5, 21).

In conclusion, mild bile duct dilatations after RFA are clinically negligible and need not be regarded as a complication. However, bile duct dilatations affecting two or more hepatic subsegments should be regarded as a major complication of RFA, which may be associated with a poorer prognosis and should be observed carefully.

© 2010 John Wiley & Sons A/S